EVALUATION OF CHROMIUM-FREE ALTERNATIVE COATINGS FOR AIRCRAFT ENGINE APPLICATIONS

Leanne Petry, Douglas C. Hansen, Christopher A. Joseph, and John J. Ruschau
University of Dayton Research Institute (UDRI)
Materials Engineering Division
Dayton, OH 45469

Chad N. Hunter
Air Force Research Laboratory
System Support Division (AFRL/MLS)
Wright-Patterson AFB, OH 45433

ABSTRACT

This effort is focused on identifying and evaluating environmentally friendly chromium-free alternatives that are purported to meet aircraft engine performance and processing requirements and serve as "drop-in" replacement candidates to chromium-containing aluminum-ceramic coatings. Chromium is a toxic material and suspected carcinogen. The elimination of hexavalent chromium found in aluminum-ceramic coatings resolves environmental, health, and safety issues associated with the operation and maintenance of turbine engines manufactured from chromium-containing aluminum-ceramic coatings. These chromium-free replacement coatings are expected to provide improved corrosion and fatigue properties. Thus, current testing is underway to evaluate the corrosion and mechanical parameters sufficient to induce coating degradation or failure as compared to the chromium-containing control. This work will benefit not only Air Force (AF) depot facilities such as Oklahoma City Air Logistics Center (OC-ALC), but also the Naval Aviation Depots at Jacksonville (NADEP JAX) and Cherry Point (NADEP CP). Preliminary results will be reported and discussed.

Keywords: coatings, chromium, corrosion protection, mechanical properties

INTRODUCTION

Aluminum-ceramic coatings containing hexavalent chromium are currently used by original equipment manufacturers (OEM's) [i.e. Pratt and Whitney-United Technologies Corporation (P&W-UTC) and General Electric Aircraft Engines (GEAE)] and Department of Defense (DoD) depot facilities (i.e. OC-ALC, NADEP JAX, NADEP CP) to provide fouling and corrosion resistance, optimum airflow efficiencies, and an ultra-smooth sealed finish primarily for low alloy steel and stainless steel engine components (i.e. compressor disks, blades,

and vanes). Hexavalent chromium has been identified as a hazardous material of concern, and is targeted for elimination or reduction by various OEMs, DoD,and Air Force (AF) policies. The Occupational Safety and Health Administration (OSHA) is leading the process changes by planning to reduce the permissible exposure limit (PEL) value for hexavalent chromium below the current 100 $\mu g/m^3$.[1] These intiatives have necessitated identification and testing of replacement environmentally-friendly candidates for chromium-containing aluminum-ceramic coatings.

In response, a joint test protocol (JTP) was developed under the tri-service Propulsion Environmental Working Group (PEWG) to enable an evaluation of performance requirements of candidate replacement coatings. These tests were derived from engineering, performance, and operational supportability requirements, as defined by a consensus of government and industry participants. Acceptance (pass or fail) criteria were established in the test methodology. General requirements for the chromium-free "drop-in" replacement coatings are that they introduce no new hazards or personal protective equipment (PPE) and eliminate hexavalent chromium. Additionally, the replacement coatings must be commercially available, have low or no volatile organic compounds (VOCs) (<350 g/L), have a shelf life greater than 6 months and a minimum pot life of 12 hours, as well as be capable of being stripped and reapplied or "touched up" and repaired.

Burnishing (mechanically cold working) by dry grit blasting the chromium-containing or chromium-free aluminum ceramic basecoat (cured at 650°F, matte gray in color) compresses the coating rendering it conductive, galvanically active, and sacrificial (cathodically protective) to all steels.[1, 2] Additionally, improved corrosion resistance of the basecoat is obtained by applying a sealer coating (topcoat), the purpose of which is to not only enhance the smoothness (i.e. fill in the porosity) of the basecoat but also to reduce the sacrifical consumption of the basecoat, extend its corrosion protection, and act as an inert surface layer.[1] As such, this paper serves to confirm these observations by providing an independent investigation of the baseline control coating (Sermetel W® basecoat + SermaSeal 570A topcoat) [(1)] and 2 candidate materials [(Coating A = Sermetel CF 1725 basecoat + SermaSeal CF 1726 topcoat) [(1)] and (Coating B = Alseal® 5000 basecoat + Alseal 5200 topcoat) [(2)] by evaluation of salt corrosion protection and sacrificial (electrochemical) properties in a saline environment, erosion resistance, high temperature heat oxidation resistance, material and substrate incompatibilities, and mechanical properties.

EXPERIMENTAL PROCEDURE

Electrical Resistance

Electrical resistance measurements were conducted by the two participating coating vendors [(1, 2)] and were made in accordance with MIL-C-81751B[3], per paragraphs 3.5.11 and 4.6.11, for a type I, class 4 coating[3] both before and after burnishing. Five (5) 4130 steel (ST) panels (4" long x 3" wide x 0.050" thick) per baseline control and coating alternative were measured, with one measurement per panel. An acceptance criterion was less than 15 ohms per inch. Each coating system was prepared and applied, in accordance with the appropriate manufacturer's specification with a total dry film thickness less than 0.003 inches, including basecoat and topcoat, over a clean, bare or pretreated substrate. Using these specifications, the coating was applied on both the sides and edges of the panels. The coating thickness of all test panels was determined per ASTM D1186[4]. The electrical resistance test was performed to assess the strength of conductivity of the coating after burnishing the basecoat.

Salt Spray Corrosion without and with Cyclic Heat

Five (5) 4130 steel (ST) panels per each coating system prepared according to the coating specifications identified in the electrical resistance section were exposed to a 5% concentration sodium chloride salt spray following those procedures outlined in ASTM B117[5], section 4.2. Salt spray exposures were static (continuous

---

[1] Manufactured by Sermatech International, Inc., a Subsidiary of Teleflex Incorporated (USA), 155 South Limerick Road, Limerick, PA 19468-1699 / 610-948-5100

[2] Manufactured by Coatings for Industry, Inc. 319 Township Line Road, Souderton, PA 18964 / 215-723-0919

for 168 or 500 hours, without heat) or cyclic (intermittent, with one cycle consisting of 16 hours continuous salt spray exposure followed immediately by 6 hours exposure to an elevated temperature of 750°F). Cyclic exposures were performed for a total of 10 cycles, with the panels cooled for 2 hours before the next cycle.

The salt spray accelerated corrosion test was performed to provide a laboratory indicator of the corrosion resistance of the coating. A small percent of engine applications call for unburnished coatings that provide only a barrier (i.e. no sacrificial properties). The cyclic test was performed to determine the coating's corrosion resistance and sacrificial capabilities under high temperature conditions. The panels were removed from the test chamber, rinsed with ASTM D1193[6] Type IV deionized water (DIW), examined for corrosion, and photographed daily throughout the duration of the static or cyclic test and results noted. Numerical ratings were assigned to the panels based on the amount of corrosion present in the scribe, the degree of undercutting (loss of adhesion) around the scribe, and the extent of blistering in the coating, if applicable. Corrosion severity was to be comparable or less than the baseline control coating.

Unburnished coated panels (basecoat without topcoat) with no scribe mark were exposed statically in salt spray for 168 hours (7 days without heat) while burnished scribed coated panels (basecoat without and with topcoat) were exposed statically in salt spray for 500 hours (21 days without heat) or cyclically in salt spray for 10 cycles as previously described. Burnishing of the basecoat was performed at the site of manufacturer with 100-250 mesh aluminum oxide (Al_2O_3) grit at 5-10 psi air pressure. The panel coating thickness, surface finish, and electrical conductivity were recorded both before and after burnishing. In some cases, after burnishing, a chromium-free topcoat was applied to the panel for a total thickness of up to 0.003 inches. An "X" was scribed into the burnished panels (without and with topcoat) through the entire coating system down to the substrate using a Hermes Gravostyle Model IS6000 Engraver equipped with diamond tipped cutting tool under computer control at the test laboratory.

Erosion

Fifteen (15) 4130 steel (ST) panels per each coating system (burnished basecoat with topcoat) were tested for erosion resistance in the form of abrasion resistance (ASTM D968[7], Method A) using a Falling Sand tester (5 ST panels per each coating system), chipping resistance (ASTM D3170[8]) using a Gravelometer (5 ST panels per each coating system), and particle erosion resistance using a novel design technique[9] (5 ST panels per each coating system). The abrasion resistance test was performed with a measured amount of certified silica sand dropping through the Falling Sand tester to initiate erosion which was continued until a spot 4 mm wide had penetrated the topcoat and exposed the basecoat-substrate layer. The coupons were placed at a 45° angle to the tester in a 76°F and 48% relative humidity environment. Chipping resistance was also investigated at 76°F and 48% relative humidity to identify the failure mechanism of the coating. Intercoat adhesion was defined as failure at the coating-substrate interface (adhesive failure), whereas intracoat adhesion was defined as failure within the coating layer itself (cohesive failure). Particle erosion resistance was conducted with silica sand ranging between 88-105 μm in size at a 30° impact angle. Mass loads of 1.0, 2.0, and 3.0 g/cm^2 at a nominal speed of 100 mph and mass loads of 0.125, 0.250, 0.500, and 1.0 g/cm^2 at a nominal speed of 300 mph were used for testing. All results were recorded and any erosion noted. Erosion resistance criteria were equivalent or better than the baseline control coating. As airfoils are the main engine components affected by erosion, this testing attempted to determine the coating's resistance to abrasion produced by abrasives impinging onto or into the coatings. Collectively, these tests were conducted to evaluate their utility and viability in assessing the erosion protection capabilities of aluminum-ceramic coatings.

Thermal Stability

Thermal stability tests were performed to evaluate coating performance in terms of thermal shock resistance and oxidation resistance at typical operation temperatures of engine components. These tests were nonstandard and were conducted as described in the JTP in an oven operated at 750°F for 100 or 500 hours. Five ST panels per coating system (burnished basecoat with topcoat) per time exposure were monitored for loss of coating, cracking, blistering or other film defects in comparison to the baseline control coating as a result of exposure.

Elevated Temperature Material Compatibility Test

The elevated temperature material compatibility test allowed assessment of substrate degradation promoted by possible material incompatibility between the coatings and dry film lubricants (DFL) or touch-up coatings or brazed alloys under high temperature conditions. In accordance with MIL-L-46010[10], the DFLs used for testing were Molydag 254 (DFL-1) and Everlube 9002 (DFL-2). The ambient cure touch-up coating used for testing was recommended by the individual manufacturer of each coating system and was not designed to be corrosion resistant. The brazed alloy used was PWA 996 Rev.E (13.0% Cr, 4.5% Si, 4.0% Fe, 2.9% B, 75.6% Ni) and was applied directly to the ST panels.

Twenty ST panels per coating system (burnished basecoat with topcoat) were scribed with an "X" through the entire coating system down to the substrate using a diamond tipped cutting tool under computer control at the test laboratory as described previously. The panels with a one inch wide brazed alloy strip down the center were hand-scribed. The DFL or touch-up coating was then applied directly to the scribe (each on 5 ST panels). After heating in an oven for 9 ± 1 hours at 750 ± 5°F, the test panels were cooled to room temperature and visually examined. The incompatibility of any replacement coating in contact with either a DFL or touch-up coating upon exposure to elevated temperatures was noted. Material degradation was to be comparable or less than the baseline control coating.

Humidity Exposure

The humidity exposure was performed to determine the effects of water ingress and subsequent degradation of the replacement coatings in comparison to the baseline control coating. Since most of the coated engine parts are stored in and exposed to high humidity environments, it was necessary to analyze the chromium-free alternative coatings' resilience against humidity and water absorption (i.e. condensing humidity). Testing was performed per a modified version of ASTM D2247[11]. Instead of the procedure specified in section 3.1 of the standard, the six ST panels per coating system (burnished basecoat with topcoat) per time exposure were placed in an enclosed Lunaire Limited (Tenney Environmental, Model T10RC) humidity chamber at a relative humidity (RH) of 95% and temperature of 140°F for 10, 20, and 30 day intervals. Panels were weighed to the nearest 0.00001g prior to testing and after 10, 20, and 30 days of testing. At each interval, the panels were removed from the humidity chamber, weighed (after drying in a 140°F oven for one hour) for mass change (water uptake), and visually examined for any evidence of color change, coating softening or blistering (coating degradation), loss of coating adhesion (coating failure), or cracking and embrittlement in comparison to the baseline control coating. Additionally, to monitor coating hardness, pencil hardness measurements were performed prior to exposure and after 30 days of testing on one of the six panels per coating system in accordance with ASTM D3363[12].

Fluid Immersion

This test assessed the susceptibility of the aluminum-ceramic coating alternatives and baseline coating to degradation and/or loss of adhesion due to contact with the fluids listed in Table 1.[13-19] Prior to immersion, the panels were visually examined under normal work lighting and 3X magnification to verify that the applied coating was a smooth film of uniform color, with no cracks, sags, runs, scratches, pinholes, blisters, nodules, or chipping. Panel weights were measured to the nearest 0.00001 g. Three ST test panels per coating system (burnished basecoat with topcoat) per fluid were immersed in a sealed glass container to a depth of 50% in the specified fluids for the indicated period of time and temperature as stated in Table 1. Once removed from the immersion exposure, panels were drained for ten minutes, triple rinsed in the appropriate solvent (Table 1), and dried in a 140°F oven for one hour. Test panels were re-weighed for fluid uptake and visually examined under 10X magnification for the coating defects in the a fore mentioned text.

Strippability

The alternative coatings must be able to be removed from the engine component substrate for routine maintenance. For aluminum-ceramic coating systems, a 30%:70% by weight sodium hydroxide (NaOH) in water solution at 180-200°F for 20-30 minutes is typically used for coating removal. The individual coating manufacturers specified a different removal process for their chromium-containing and chromium-free coating systems. Five ST test panels per coating system (burnished basecoat with topcoat) were stripped per the procedures outlined in Table 2.

Hydrogen Embrittlement

Hydrogen (H_2) embrittlement testing was performed on notched tensile samples coated with each coating system following those procedures outlined in ASTM F519[20]. A type 1a.1 specimen design was used to investigate embrittlement concerns of each coating system, following the protocol listed for Plating Processes, whereby a minimum of 4 samples are loaded to 75% of the notch tensile strength (NTS) in lab air for a minimum of 200 hours without failure. Samples machined from 4340 steel were provided by SMI, Inc.[(3)] along with certification of the NTS per the ASTM F519 standard. An exception to the F519 standard was that since the coated samples are required to undergo a cure cycle at approximately 650°F for typically one hour, a modified NTS was established from 5 uncoated but similarly thermally aged samples to estimate the NTS following the thermal age. In all cases, the NTS was reduced slightly from approximately 385 ksi to 325 ksi following the thermal cycle. Samples tested for H_2 embrittlement were thus subjected to 75% of this modified NTS value, using SATEC creep/stress-rupture, direct-load testing frames with a 20:1 loading ratio.

Electrochemical

Electrochemical testing consisted of measurement of open circuit potentials (OCP) and impedances (in accordance with ASTM G3[21] and ASTM G106[22]) of the baseline control coating and alternative chromium-free coating systems using one of three potentiostats (either an EG&G Model 273A, 283, or 2273) [(4)] coupled to a Solartron Model 1250 or 1260 [(5)] frequency response analyzer, or equivalent. A saturated calomel electrode (SCE) was used as the reference electrode (RE), and the testing apparatus was a coating cell manufactured by Scribner Associates [(6)] with a 13 cm^2 exposed surface area filled with approximately 100 mL of 3.5% sodium chloride (NaCl) solution prepared with deionized water (per ASTM D1193[4] Type IV) as the electrolyte. A platinum mesh was used as the counter electrode, and the working electrode was either an uncoated ST panel or a ST panel with burnished basecoat in the topcoated or nontopcoated condition. Measurements were made in triplicate on separate unscribed panels. The open circuit potential was monitored for 24 hours prior to initiation of the impedance measurement taken at 0 V versus the OCP. For impedance measurements, the frequency sweep was started at a high frequency of either 100,000 hertz or 65,000 hertz (instrument dependent) and ramped to a low frequency of 0.01 hertz using a 10 mV amplitude and a data interval of log 10 steps/decade. The OCP was measured for 24 hours to ensure equilibrium had been obtained prior to the electrochemical impedance spectroscopy (EIS) measurements. Electrochemical impedance enabled an assessment of the polarization resistance provided by the individual coating systems.

RESULTS

Electrical Resistance

It was discussed earlier that the coating systems, specifically the basecoat, must be made electrically conductive to obtain sacrificial properties. This was done by burnishing with aluminum oxide and verified using light pressure with probes of a standard ohm meter placed 1” apart. The JTP set an acceptance criterion of less than 15 ohms per inch. The conductivity of all post burnished coating systems (measured without and with application of sealing topcoat) measured 0 ohms, well below the acceptable criterion. The basecoat thicknesses ranged from 1.8-2.5 mils with surface roughnesses (Ra) of 31-56 prior to burnishing. After burnishing, the basecoat thicknesses and surface roughnesses were 1.7-2.1 mils and 45-85 Ra, respectively. Thus, the burnishing process made the basecoats more compact and rougher. Application of the topcoat sealer increased the total coating thickness to 1.8-3.5 mils, which was within the specified total dry film thickness. The surface roughness after topcoating was measured to verify a sealed finish smoother than (less than) an Ra of 45-56. The measured

[3] SMI, Inc., FL

[4] Princeton Applied Research, Oakridge, TN 37831

[5] Solartron Analytical, Hampshire, UK GU14 ONR

[6] Scribner Associates, Southern Pines, NC 28387

Ra was 24.1-43.9, 20.9-35.9, and 42.0-43.5 for the baseline control, Coating A, and Coating B topcoated systems, respectively.

Salt Spray Corrosion without and with Addition of Heat Cycle

Optical photographs were taken of representative panels from each coating system and exposure condition (static or cyclic salt fog) after testing and are shown in Figures 1 through 5. Visual observation of Coating B indicated that the nonscribed unburnished basecoat did not provide corrosion protection as well as either the baseline control or Coating A nonscribed unburnished basecoat when exposed for 168 hours to an ASTM B117[5] salt fog environment (Figure 1). Coating B had heavy rust (iron oxide, staining) buildup, streaking, and staining on the surface of the panel. The baseline control and Coating A were mottled with water spots and some rust staining. Removal of the basecoat on a representative panel from each unburnished basecoat system using the procedures outlined in Table 2 revealed under 10X magnification no pitting or indication of rusting of the 4340 substrate for the baseline control and Coating A but rust staining, blistering, and pitting of the 4340 substrate for Coating B. This observation suggested unburnished Coating B did not provide barrier protection as well as the unburnished baseline control or Coating A.

To evaluate corrosion in the burnished scribed coated panels (basecoat without and with topcoat) after 500 hours static salt fog exposure, the rating scale in Table 3a was used. Numerical ratings (Table 3b) were assigned to the panels based on the amount of corrosion present in the scribe, the degree of undercutting (loss of adhesion) around the scribe, and the extent of blistering in the coating, if applicable. The burnished and scribed basecoat panels (without topcoat) rated 3 (moderate corrosion product buildup), 0 (no undercutting), 10 (no blistering) for each coating system (Figure 2), while addition of the topcoat to the burnished panels improved the scribe rating in all cases to 2 (minor corrosion product buildup), 0, 10 (Figure 3). These ratings suggested the chromium-free alternative coating systems offered corrosion resistance comparable to the chromium-containing baseline control coating system when exposed to an ASTM B117[5] salt fog environment.

The same rating scale as shown in Table 3a was used to evaluate corrosion in the burnished scribed coated panels (basecoat without and with topcoat) after 500 hours cyclic salt fog exposure (addition of an elevated temperature exposure). These panel ratings are listed in Table 3b as well. The basecoat of the baseline control (burnished, scribed, and without topcoat) rated 1 (staining and no corrosion product buildup), 0, 10, where as the basecoat for Coatings A and B rated poorer in the scribe at 2, 0, 10 (Figure 4). Surprisingly, the ratings of Coatings A and B with topcoat remained unchanged after cycle exposure (2, 0, 10). The baseline control did not fair as well with the addition of a topcoat in the cyclic exposure. These panels had minor corrosion product buildup in the scribe (2) with no undercutting (0) and no blistering (10). Thus, all topcoated systems rated similarly and there was not much differentiation between the three coating materials' sacrificial capabilities under high temperature conditions (Figure 5). This suggested the addition of the topcoat and or the addition of heat cycles with salt exposure did not impact corrosion performance. Again, these results indicated that the two chromium-free alternatives offered corrosion resistance comparable to the chromium-containing baseline control. Of interest is the visual comparison of the scribes among the topcoated systems from the static and cyclic exposures. For the topcoated baseline control and Coating A systems, the appearance of rust or staining was much greater and the amount of corrosion product buildup was much less in the cyclic exposure than in the static (no heat) salt fog exposure. Coating B had a significant amount of corrosion product buildup and some staining from the static exposure. These observations were not as pronounced in the cyclic exposure. Because of the inherent difference between the static and cyclic exposure environments, no correlation could be drawn for each coating system between exposure environments.

Using a JEOL [(7)] model JSM-6460 LV low vacuum scanning electron microscope (SEM) equipped with an EDAX [(8)] Genesis energy dispersive spectroscopy (EDS) system, bulk chemical analysis was performed to identify the corrosion product and staining composition responsible for the ratings of 2 and 3 given previously. In order of appearance Figures 6a, 7a, and 8a show the SEM images of the baseline control coating, Coating A, and

[7] JEOL USA, INC., 11 Dearborn Rd P.O. Box 6043, Peabody, MA 01961-6043/978-535-5900

[8] EDAX, Inc., 91 McKee Drive, Mahwah, NJ 07430

Coating B, all in the burnished basecoat, topcoated, and scribed condition after 500 hours salt fog exposure. These images were taken at 10keV in backscatter mode at a magnification of 30X and a working distance of 11mm. The dark (black arrows) and light (gray arrows) areas present in the images of the scribes are indicative of lighter and heavier elements, respectively. The EDS spectra for the dark and light areas of each respective SEM image are shown in Figures 6b, 7b, and 8b. In all cases, the dark areas of the scribe are identified to be aluminum oxide corrosion product, probably resulting from environmental degradation of the aluminum ceramic coating. The light areas of the scribe are indicated to be iron oxide corrosion product or staining, indicative of corrosion of the 4130 steel substrate. The presence of chromium is noted in the scribe of the baseline control (Figure 6b). This signifies that the inhibitor is leaching out of the coating to provide protection at a defect site (scribe).

Removal of the complete coating system using the procedures outlined in Table 2 on a representative panel from each scribed burnished basecoat plus topcoat system from the static salt fog exposure revealed under 10X magnification no pitting or indication of rusting in the scribe of the 4130 substrate for the baseline control or Coating A but rust staining, rust blisters, and pitting of the 4130 substrate for Coating B. This observation suggested the burnished Coating B did not provide the barrier protection that the burnished baseline control and Coating A provided.

Erosion

According to MIL-C-81751B[3] the abrasion resistance shall be such that when tested with falling sand, the abrasion coefficient (liters of sand per mil of thickness) of a type I coating cured at 650°F shall not be less than 100. ASTM D968[7] specifies performing the abrasion resistance test until a spot 4 mm wide was penetrated. In all cases, this size spot was reached upon erosion of the topcoat and exposure of the basecoat-substrate layer. The results of the Falling Sand test are given in Table 4 and are recorded as liters per mil of topcoat thickness. Figure 9 shows the optical photographs for each topcoated system (burnished basecoat). Three spots were tested on each panel with the filmbuild (total coating thickness) recorded prior to the test and the amount of topcoat abraded determined after testing. Although the measured abrasion coefficient is significantly less than 100 (actually measured to be 2.0-8.2), it can be determined that the topcoat of Coating A had the best performance (indicated by the highest value in Table 4) followed by the topcoat of the baseline control coating. The topcoat of Coating B had the least amount of abrasion resistance. This indicated that the topcoat of Coating A was more durable than the other coatings and was more resistant to erosion.

To evaluate the chipping resistance of the different coating systems (burnished basecoat with topcoat), the rating scale in Table 5 was used. Alpha numerical ratings were assigned to the panels based on the number of chips present in the coating, the size of the chips present in the coating, and the point of failure in the coating. The extent of damage incurred by each coating system after being subjected to the gravelometer is shown in Figure 10. All three systems rated 1 (150-250 chips), A (chips < 1mm in size), T (cohesional failure at the topcoat). This meant that for all coating systems evaluated for chipping resistance, the predominant failure mechanism was identified to be intracoat adhesion (cohesive failure) at the topcoat layer. It is possible that this is due to an extremely strong bond between the surface of the substrate and the aluminum ceramic basecoat or that the basecoat is harder than the topcoat and has more of an ability to resist strong impacts such as those caused by the gravelometer. Collectively, these ratings suggested the chromium-free alternative coating systems offered chipping resistance comparable to the chromium-containing baseline control coating system when subjected to flying debris.

Optical photographs of the chromium-free alternative coatings (Coatings A and B) are shown in Figure 11 after particle erosion testing at nominal speeds of 100 mph (Figure 11a) and 300 mph (Figure 11b). Evident in the photographs is the erosion (wearing away) of the topcoat and exposure of the basecoat. Not evident in the photographs, but visible under 10X magnification, is the evidence of basecoat penetration and 4340 steel substrate exposure. Plots of the panel mass loss (indicative of coating erosion) versus mass load of sand for each coating system at each speed tested are shown in Figure 12. For mass loads of sand between 1-3 g/cm^2 at a calibrated speed of 118 mph (Figure 12a), there is a linear erosion (mass loss) of each coating system. The same linear trend is true for mass loads of sand between 0.125 and 0.500 g/cm^2 at a calibrated speed of 308 mph (Figure 12b). Additionally, it is noted that for both speeds, Coating B appears to be losing more mass than either Coating A or the baseline control. This may be due to differences in coating formulation and density and does not necessarily imply that one coating is more erosion resistant than another. There also appears to be the attainment of a second

regime, after the linear region, which is indicated by the stabilization of mass loss. There is not enough evidence available at this time, however, to indicate whether this is due to thinning of the basecoat or substrate material.

Thermal Stability

The 100 and 500 hour exposures of each coating system at 750°F showed no apparent damage (i.e. no blistering, softening, or other form of coating degradation or failure). Visually, there was a slight overall darkening (possible oxidation initiation) of Coating A due to the temperature exposure, but this discoloration is not sufficient cause for rejection. The baseline control coating and Coating B looked unchanged.

Elevated Temperature Material Compatibility Test

The elevated temperature material compatibility test allowed assessment of substrate degradation promoted by possible material incompatibility between the coatings and dry film lubricants (DFL), cosmetic touch-up coatings, or brazed alloys under high temperature conditions. In all cases, the tendency of any replacement or baseline coating (all systems tested were burnished basecoat with topcoat) coming into contact with either DFL or touch-up coating did not appear to promote any material incompatibilities at elevated temperatures. Application issues were noted with the DFLs in the form of adhesion or blistering of the DFL. However, the topcoat, the basecoat, and the scribe remained unaffected. Only a basecoat touch up as recommended by the manufacturer was used for the baseline control and Coating A. A basecoat touchup and a basecoat plus topcoat touchup were recommended and tested for Coating B. Additionally, the panels with a one inch wide brazed alloy strip under the coating stackup but on top of the substrate remained clean and bright in the scribe after oven heating. Thus, the incorporation of a brazed alloy into the system did not seem to contribute to any sort of material degradation.

Humidity Exposure

Since most of the coated engine parts are stored in and exposed to high humidity environments, it was necessary to analyze the chromium-free alternative coatings' resilience against humidity and water absorption (i.e. condensing humidity). Additionally, weather conditions, specifically humidity and temperature fluctuations, during engine operation may change the color characteristics of the aluminum ceramic basecoat or complete coating system. Thus, humidity exposure of the complete coating system was performed to determine the effects of water ingress and subsequent degradation of the replacement coatings in comparison to the baseline control coating.

Panels were weighed to the nearest 0.00001g prior to testing and the uptake of water after 30 days of testing was recorded as a mass gain (Table 6). Interestingly, Coating A (burnished basecoat plus topcoat) took on the most water (164 mg). The baseline control coating and Coating B gained only 2 and 3 mg, respectively. Visually, Coating A had evidence of color change in terms of increased dark mottling and a patchy film (possibly a biofilm) on the topcoat. Minor pitting was observed. The baseline control remained relatively unchanged after 30 days exposure, with the exception of increased staining of the topcoat. Coating B exhibited water spots and streaking in addition to off-white deposits on the surface of the topcoat. These observations are also noted in Table 6 and are shown in Figure 13.

To monitor coating hardness, pencil hardness measurements (gouge and scratch) were performed prior to humidity exposure and after 30 days of testing on one representative panel per coating system in accordance with ASTM D3363[12]. Pencil hardness was measured using Sanford Turquoise Drawing Leads. The coated test panel was placed on a firm and level horizontal surface. The testing was started with the hardest pencil (6H) holding it at a 45° angle to the surface of the test panel. A uniform downward and forward pressure was exerted to move the lead forward ¼ inch. The surface and lead tip were then examined to see if the coating was cut or scratched, or if the edge of the lead crumbled or left a trace marking on the coating. The process was repeated down the hardness scale until the pencil no longer cut into or gouged the coating, which was defined as the pencil hardness. The full set of leads contained the following hardness designations: 6B (softest), 5B, 4B, 3B, 2B, B, HB, F, H, 2H, 3H, 4H, 5H, 6H (hardest). The gouge hardness or film rupture was greater than 6H in all cases prior to (time zero) and after humidity exposure (30 days). Similarly, the scratch resistance of the baseline control and Coating B was greater than 6H for both time intervals. In contrast, Coating A had an initial scratch resistance of HB and a final scratch resistance of H.

Fluid Immersion

This test assessed the susceptibility of the topcoated aluminum-ceramic burnished coating alternatives and baseline coating to degradation and/or loss of adhesion due to contact with the fluids listed in Table 1.[13-19] Turbine engine components are known to come into contact with these aircraft fluids. Prior to immersion, the panels were visually examined under normal work lighting and 3X magnification. There was some particle debris on and scratches in the surface of the baseline control. Coating A appeared very porous, while Coating B appeared to have no apparent coating defects. Once removed from the immersion exposures, panels were drained for ten minutes, triple rinsed in the appropriate solvent (Table 1), and dried in a 140°F oven for one hour. Test panels were re-weighed for fluid uptake and visually examined under 10X magnification for signs of wrinkling, blistering, pitting, or other coating defects.

The fluid uptake values and post-test visual observations are noted in Table 7. The baseline control coating showed no apparent damage after immersion in any of the test fluids. It did however exhibit a mass gain in every case. The least amount of fluid uptake was noted for both the distilled water and anti-icing fluid. The two largest uptakes occurred after immersion in the lubricating oils. The chromium-free alternatives had mixed visual observations from no apparent damage and little fluid uptake in the aircraft jet fuels to coating discoloration and staining as in the case of Coating A or significant mass loss (> 75 mg) or significant mass gain (> 100mg) in the case of Coating B. Figures 14 and 15 show the range of damage noted for each coating system after immersion in either the hot distilled water and one of the hot engine lubricating oils, respectively.

Of significant interest are the visual observations shown in Figures 14c and 15c for Coating B. In Figure 14c, the topcoat removal above the 50% immersion line is evident. Upon closer examination, it is apparent in the SEM backscatter image and EDS spectra of Figure 16 that the darker area is the aluminum oxide basecoat and the lighter area is the topcoat sealer (primarily cobalt titanate). These color contrasts are reversed in the optical photograph of Figure 14c, and the microscopy results confirm the absence of the topcoat. The manufacturer notes that hot water vapor solubilization of the topcoat may occur in cases of incomplete topcoat cure.

Similarly, upon closer examination of the off-white chalky deposits identified in Figure 15c, a contrast in elemental density is noted in the SEM backscatter image of Figure 17a. However, EDS interrogation of both the light and dark areas of the image revealed that there was a thin film residue over the entire surface of the cobalt titanate topcoated panel that was exposed to hot oil vapors. Spectra from both areas were identical and revealed not only the topcoat signature peaks but also a large silicon peak most likely attributed to a silicon additive incorporated into the oil formulation to act as a defoamant.[23] Additionally, it is noted in MIL-C-81751B[3] that the coating systems should withstand immersion in oil at a temperature of 250°F for 24 hours without showing surface defects. The lubricating oil immersion tests executed in this evaluation were performed at 400°F for 8 hours and show evidence of product buildup or residue.

Unfortunately, when compared to the chromium-containing baseline control, both alternative chromium-free coatings were affected to varying degrees by these common aircraft fluids. It was determined that certain fluids impacted the coating systems in a detrimental way that may have resulted in objectionable alteration of the surface (i.e. discoloration, softening, swelling, build up, or loss of adhesion).

Strippability

The alternative coatings were evaluated on their ability to be removed from the engine component ST substrate for routine maintenance. The JTP set a stripping criteria of 20-30 minutes for coating removal. Both coating manufacturers' processes[24, 25] were less aggressive (baseline control and Coating A used 120 g/L NaOH at 160-180°F, while Coating B used 10% NaOH solution at 150°F) than the recommended 30% NaOH solution at 180-200°F. The coating removal procedure for the baseline control was also used for Coating A since the manufacturer did not specify separate procedures for the chromium-containing versus chromium-free aluminum ceramic coatings.

Neither manufacturer specified a "time to strip" in their data sheet. Fortunately, all coatings met the criteria of being removable (Figure 18); however, only Coating A met the additional criteria of being removed in 20-30 minutes. Coating A was actually removed after 15 minutes of complete immersion. Coating B required 75 minutes, whereas the baseline control needed a total of 120 minutes complete immersion. Visual observations

taken from the removal process are noted in Table 2. Of special interest is the high degree of vigorous bubbling produced by the immersion solution as a result of hydrogen and aluminum metal powder generation.

Hydrogen Embrittlement

The results of hydrogen embrittlement testing on 4 samples each coated with either the baseline control coating, Coating A, or Coating B showed no failures after 200 hours for samples loaded to 75% of the modified NTS. These results suggested that there were no embrittlement concerns under the conditions evaluated for any of the candidate coating systems as applied to high strength steel.

Electrochemical

To further evaluate the performance of the aluminum ceramic coatings, electrochemical parameters other than conductivity, such as the OCP and Rp, were measured. Table 8 reports the 24 hour equilibrium potential relative to a SCE in a 3.5% sodium chloride solution. This was done to ensure that the coating-substrate system was at equilibrium prior to making the impedance measurement. Electrochemical impedance spectroscopy (EIS) enabled an assessment of the corrosion resistance provided by the individual coating systems. The polarization resistance (Rp) in the aluminum ceramic coatings was calculated by examining the difference between the measured impedance at sufficiently high and low frequencies in the complex plane. From that difference, it was possible to determine that relative to the uncoated 4130 steel substrate, all burnished basecoats with and without topcoats provided better corrosion resistance or higher Rp values (Table 8). Overall, the baseline control (burnished basecoat plus topcoat) had the highest Rp value at $3.3x10^6$ ohms-cm. The burnished basecoat of Coating B had the lowest Rp value ($2.6x10^4$ ohms-cm). Of the untopcoated burnished basecoats, the baseline control provided a higher Rp ($9.6x10^5$ ohms-cm) relative to the 4130 bare steel ($7.0x10^3$ ohms-cm).

CONCLUSIONS

Although chromium-containing aluminum-ceramic coatings offer the desired galvanic corrosion protection for aircraft engine applications, overall the chromium-free “drop-in” replacement coatings offered corrosion resistance comparable to the chromium-containing baseline control coating system when exposed to an ASTM B117[3] salt fog environment. The addition of heat cycles with salt exposure did not appear to negatively impact corrosion performance. Furthermore, the tendency of any replacement or baseline coating coming into contact with either a dry film lubricant, a touch-up coating, or a braze alloy did not appear to degrade or to promote corrosion or any material incompatibilities at elevated temperatures. Oxidation tests performed at 750°F for up to 500 hours indicated thermal stability. These corrosion, lubricity, and oxidative results concurred with earlier findings.[1, 2] Erosion results showed degradation of the topcoat and are currently inconclusive for the basecoat layer or basecoat-substrate interface. Additionally, all coatings met the criteria of being completely removable; however, only Coating A met the specified criteria of being removed in 20-30 minutes using the procedures outlined in this paper. Unfortunately, when compared to the chromium-containing baseline control, both alternative chromium-free coatings were effected to varying degrees by common aircraft fluids used for immersion testing purposes. It was determined that certain fluids impacted the chromium-free replacements in a detrimental way that may have resulted in objectionable alteration of the surface (i.e. discoloration, softening, swelling, build up, or loss of adhesion).

The chromium-free alternatives were impacted by humidity exposure, namely in the form of water absorption and hardness change (Coating A) or topcoat solubility (Coating B). The conductivity of all post burnished coating systems (measured without and with application of topcoat sealer) was well below the acceptable criterion of 15 ohms per inch, and therefore, were quite conductive. All burnished basecoats with and without topcoats provided better corrosion resistance or higher Rp values relative to the 4130 steel substrate.

On-going work is evaluating corrosion severity and coating thermal stability at longer exposure times (750°F for 1000 hours or at 1000°F for 100 hours). Any failed panels from the thermal stability test will be cut and evaluated for oxidation at the substrate-coating interface per ASTM E3-01[26]. Chromium-free alternative coatings applied to substrates of 410, A286, IN718 will also be tested for thermal stability. Each thermally tested material (ST, 410, A286, IN718) will then be evaluated for surface profilometry (surface roughness) and adhesion (per ASTM B571[27] and Section 4.9). Panels from the materials compatibility testing will also be examined

metallographically per ASTM E3-01[26]. The JTP participants agreed that it is important to assess the tendency, if any, of a candidate coating in contact with either DFL, touch-up coating, or braze alloy to promote corrosion [specifically intergranular attack (IGA)] at elevated temperatures.

Future mechanical testing is to address adherence issues of candidate coating systems or debits in substrate performance including qualitative adhesion testing per ASTM B571[27] using the bend test approach (90° bend); constant amplitude fatigue following ASTM E466[28]; and stress corrosion cracking using the direct load method described in ASTM G47[29] for a 3.5% NaCl constant environment. Hydrogen embrittlement results suggested that there were no embrittlement concerns under the conditions evaluated for any of the candidate coating systems as applied to high strength steel.

ACKNOWLEDGMENTS

This work was performed under the United States Air Force contract number F33615-03-D-5607. The authors would like to thank Dr. Paul L. Ret (AFRL/MLSA), Steven R. Thompson (AFRL/MLSC), and Tom S. Pagnard (PRSS/YN) for their technical oversight, and the UDRI Materials Engineering Division Technical Staff for their laboratory expertise, particularly Mr. Elmer R. Baldwin, Mr. Charles M. Blair, Mr. John E. Buhrmaster, Mr. John R. Conner, Mr. John G. Stalter, and Mr. Roger L. Vissoc.

REFERENCES

1. Mosser, M.F. “Progress on Environmentally Compliant Aluminum Ceramic Compressor Coatings.” Proceedings of ASME Turbo Expo 2004. Vienna, Austria. June 14-17, 2004.
2. Mosser, M.F. “Compressor Disk Corrosion: Problems and Solutions.” SAE Technical Paper at the 25th Annual Aerospace/Airline Plating and Metal Finishing Forum & Exposition. New Orleans, LA. March 27-30, 1989.
3. MIL-C-81751B Military Specification, Coating, Metallic-Ceramic. 17 January 1972.
4. ASTM D 1186-01 Standard Test Methods for Nondestructive Measurement of Dry Film Thickness of Nonmagnetic Coatings Applied to a Ferrous Base. American Society for Testing and Materials.
5. ASTM B 117-03 Standard Practice for Operating Salt Spray (Fog) Apparatus. American Society for Testing and Materials.
6. ASTM D 1193-99 Standard Specification for Reagent Water. American Society for Testing and Materials.
7. ASTM D 968-93 (Reapproved 2001) Standard Test Methods for Abrasion Resistance of Organic Coatings by Falling Abrasive. American Society for Testing and Materials.
8. ASTM D 3170-03 Standard Test Method for Chipping Resistance of Coatings. American Society for Testing and Materials.
9. Blair, C.M. “Upgrading the Air Force Research Laboratory (AFRL) Particle Erosion Test Facility.” Joint DoD/FAA/NASA Conference on Aging Aircraft Proceedings. Palm Springs, CA. January 31- February 4, 2005.
10. MIL-PRF-46010F Performance Specification, Lubricant, Solid Film, Heat Cured, Corrosion Inhibiting. 10 August 2000.
11. ASTM D2247-02 Standard Practice for Testing Water Resistance of Coatings in 100% Relative Humidity. American Society for Testing and Materials.
12. ASTM D3363-05 Standard Test Method for Film Hardness by Pencil Test. American Society for Testing and Materials.

13. MIL-PRF-7808L Performance Specification, Lubricating Oil, Aircraft Turbine Engine, Synthetic Base. 2 May 1997.
14. MIL-PRF-23699F Performance Specification, Lubricating Oil, Aircraft Turbine Engine, Synthetic Base, NATO Code Number O-156. 21 May 1997.
15. AMS 1424F Aerospace Material Specification, Deicing/Anti-Icing Fluid, Aircraft SAE Type 1. May 2005.
16. AMS1435A Aerospace Material Specification, Fluid, Generic, Deicing/Anti-Icing Runways and Taxiways. August 1999.
17. MIL-T-83133D Military Specification, Turbine Fuels, Aviation, Kerosene Types, NATO F-34 (JP-8) and NATO F-35. 29 January 1992.
18. MIL-PRF-5606H Performance Specification, Hydraulic Fluid, Petroleum Base; Aircraft, Missile, and Ordnance. 7 June 2002.
19. MIL-PRF-83282D Performance Specification, Hydraulic Fluid, Fire Resistant, Synthetic Hydrocarbon Base, Metric, NATO Code Number H-537. 30 September1997.
20. ASTM F519-05 Standard Test Method for Mechanical Hydrogen Embrittlement Evaluation of Plating/Coating Processes and Service Environments. American Society for Testing and Materials.
21. ASTM G3-89 (Reapproved 2004) Standard Practice for Conventions Applicable to Electrochemical Measurements in Corrosion Testing. American Society for Testing and Materials.
22. ASTM G106-89 (Reapproved 2004) Standard Practice for Verification of Algorithm and Equipment for Electrochemical Impedance Measurements. American Society for Testing and Materials.
23. http://www.lube-tips.com/BackIssues/2001-7-26.htm.
24. Sermatech Lab Procedure 92-1 for Chromated Coatings.
25. Alseal 5000® Product Data Sheet (rev. 5-02).
26. ASTM E3-01 Standard Guide for Preparation of Metallographic Specimens. American Society for Testing and Materials.
27. ASTM B571-97 (Reapproved 2003) Standard Practice for Qualitative Adhesion Testing of Metallic Coatings. American Society for Testing and Materials.
28. ASTM E466-96 (Reapproved 2002) Standard Practice for Conducting Force Controlled Constant Amplitude Axial Fatigue Tests of Metallic Materials. American Society for Testing and Materials.
29. ASTM G47-98 (Reapproved 2004) Standard Test Method for Determining Susceptibility to Stress-Corrosion Cracking of 2XXX and 7XXX Aluminum Alloy Products. American Society for Testing and Materials.

Table 1. Fluid Immersion Test Matrix.

Immersion Fluid	Reference Document	Rinse Solvent	Immersion Exposure Time and Temperature
Aircraft Engine Lubricating Oil	MIL-L-7808[11]	Naptha	8 Hours at 400°F
Aircraft Engine Lubricating Oil	MIL-L-23699[12]	Naptha	8 Hours at 400°F
Anti-Icing Fluid, Octoflo EF-50/50 Dilution	AMS 1424E[13]	Distilled Water	24 Hours at Room Temperature
Runway Deicing Fluid, Cryotech E36 LRD	AMS1435[14]	Distilled Water	24 Hours at Room Temperature
Aircraft Fuel, JP-4	MIL-T-83133D[15]	Naptha	24 Hours at Room Temperature
Aircraft Fuel, JP-8	MIL-T-83133D[15]	Naptha	24 Hours at Room Temperature
Distilled Water (Type III)	ASTM D1193[4]	None	24 Hours at 120°F
Hydraulic Fluid, Skydrol	Not Applicable	Naptha	24 Hours at Room Temperature
Hydraulic Fluid	MIL-H-5606[16]	Naptha	24 Hours at Room Temperature
Hydraulic Fluid	MIL-PRF-83282[17]	Naptha	24 Hours at Room Temperature

Table 2. Coating Removal Procedures.

Baseline Control Coating	Coating A	Coating B
120 g/L NaOH at 160-180°F	120 g/L NaOH at 160-180°F	10% by Weight NaOH at 150°F
Immerse coated panel in solution	Immerse coated panel in solution	Immerse coated panel in solution
No set time limit*	No set time limit	No set time limit
Scrubbed with a medium tampico brush under warm running water**	Scrubbed with a medium tampico brush under warm running water	Scrubbed with a medium tampico brush under warm running water
Rinsed with ethanol**	Rinsed with ethanol	Rinsed with ethanol
Blown dry with nitrogen gas to prevent flash rusting of the steel substrate**	Blown dry with nitrogen gas to prevent flash rusting of the steel substrate	Blown dry with nitrogen gas to prevent flash rusting of the steel substrate
Grit blast any remaining residue***	Grit blast any remaining residue	Grit blast any remaining residue
Process Observations	**Process Observations**	**Process Observations**
Initial solution lost effectiveness after 60 minutes and was replaced	Vigorous bubbling (hydrogen generated) for 1st 5 minutes of immersion	Vigorous bubbling (hydrogen generated) for 1st 5 minutes of immersion
Cessation of bubbles at 115 minutes	Cessation of bubbles at 15 minutes	Green topcoat removed 1st and proceeded to float in stripping solution
120 minutes total immersion time	15 minutes total immersion time	90% coating removal from flat panel face at 60 minutes
Stripped panels are grey-black in color	Stripped panels are dark, grey-black in color	75 minutes total immersion time
Coating residue (aluminum metal powder, chromates) was chalky and nearly same color as cured coating	Coating residue (aluminum metal powder) was dark and chalky	Stripped panels are light, silver-grey in color
		Coating residue (aluminum metal powder) was light in color and slight in quantity

*The Joint Test Protocol (JTP) set a striping criteria of 20-30 minutes for coating removal.

**Testing laboratory in-house procedure not called out by the coating manufacturer.

***Grit blasting was not performed by the testing laboratory as it was not called out in the JTP.

Table 3a. Salt Spray Rating Scale.

1st Digit - Scribe Appearance	
0	Bright and clean
1	Staining, minor corrosion but no build up
2	Minor/moderate corrosion product build up
3	Moderate corrosion product build up
4	Major corrosion product build up
5	Severe corrosion product build up

2nd Digit Undercutting	
0	No lifting of coating
1	Lifting or loss of adhesion up to 1/16" (2 mm)
2	Lifting or loss of adhesion up to 1/8" (3 mm)
3	Lifting or loss of adhesion up to 1/4" (7 mm)
4	Lifting or loss of adhesion up to 1/2" (13 mm)
5	Lifting or loss of adhesion beyond 1/2" (>13 mm)

3rd Digit - Blistering / ASTM D 714	
Size	**Frequency**
10 = None	F = Few
8 = Smallest	M = Medium
6 = Small to Medium	MD = Med. Dense
4 = Medium to Large	D = Dense
2 = Large	

Table 3b. Salt Spray Rating of Exposed Specimens.

Coating Condition	Exposure Environment	Scribe Appearance	Undercutting	Blistering
*Burnished Basecoat	Static salt spray, 500 hours	3	0	10
**Burnished Basecoat + Topcoat	Static salt spray, 500 hours	2	0	10
Baseline Coating Burnished Basecoat	Cyclic salt spray, 10 cycles	1	0	10
Coating A Burnished Basecoat	Cyclic salt spray, 10 cycles	2	0	10
Coating B Burnished Basecoat	Cyclic salt spray, 10 cycles	2	0	10
Baseline Coating Burnished Basecoat + Topcoat Seal	Cyclic salt spray, 10 cycles	2	0	10
Coating A Burnished Basecoat + Topcoat Seal	Cyclic salt spray, 10 cycles	2	0	10
Coating B Burnished Basecoat + Topcoat Seal	Cyclic salt spray, 10 cycles	2	0	10

* For all three nontopcoated burnished basecoat systems: baseline control, A, and B. ** For all three topcoated burnished basecoat systems: baseline control, A, and B.

Table 4. Falling Sand Results in Units of Liters per mil of Topcoat Thickness.

Baseline Control Coating	Coating A	Coating B
3.710	8.200	2.033

Table 5. Chipping Resistance Rating Scale.

1st Digit

Number of Chips	Rating	Number of Chips	Rating	Number of Chips
	10	0	4	50 - 74
	9	1	3	75 - 99
	8	2 - 4	2	100 - 149
	7	5 - 9	1	150 - 250
	6	10 - 24	0	> 250
	5	25 - 49	This Area Left Blank	

2nd Digit

Size Categories	
A	< 1 mm
B	1 - 3 mm
C	3 - 6 mm
D	> 6 mm

3rd Digit

Point of Failure Notation		
Notation	Level of Failure	Failure Type
SP	Substrate to Primer	Adhesional
ST	Substrate to Topcoat	Adhesional
P	Primer	Cohesional
PT	Primer to Topcoat	Adhesional
T	Topcoat	Cohesional

Table 6. Humidity Exposure Observations (n = 6).

Specimen	Water Uptake 30 Days	Visual Observations 30 Days
Baseline Control	Mass Gain 2 mg	Unchanged with the exception of increased staining and/or bloom of topcoat
Coating A	Mass Gain 164 mg	Increased dark mottling, pitting, patchy film on topcoat
Coating B	Mass Gain 3 mg	Water spots/streaking/off-white deposits on surface of topcoat

Table 7. Fluid Immersion Post-test Fluid Uptake and Visual Observations at 10X (n = 3).

Immersion Fluid	Baseline Control Coating	Coating A	Coating B
Aircraft Engine Lubricating Oil MIL-L-7808[11]	119 mg No apparent damage	109 mg Slight darkening	131 mg Off-white chalky deposits
Aircraft Engine Lubricating Oil MIL-L-23699[12]	35 mg No apparent damage	162 mg No apparent damage	136 mg Off-white chalky deposits
Anti-Icing Fluid, Octoflo EF-50/50 Dilution	2 mg No apparent damage	46 mg Staining, darkening	-14 mg Slight lightening, staining
Runway Deicing Fluid, Cryotech E36 LRD	20 mg No apparent damage	74 mg Mottling, lightening of coating, fluid bleeding from coating	-13 mg Slight lightening, staining
Aircraft Fuel, JP-4	7 mg No apparent damage	11 mg No apparent damage	0 mg Slight darkening
Aircraft Fuel, JP-8	16 mg No apparent damage	19 mg No apparent damage	1 mg No apparent damage
Distilled Water (Type III)	2 mg No apparent damage	16 mg Slight lightening	-76 mg Softening, removal of topcoat at air-fluid interface
Hydraulic Fluid, Skydrol	10 mg No apparent damage	9 mg No apparent damage	117 mg No apparent damage
Hydraulic Fluid MIL-H-5606[16]	6 mg No apparent damage	66 mg Fluid stained	36 mg Slight fluid stain
Hydraulic Fluid MIL-PRF-83282[17]	14 mg No apparent damage	104 mg Fluid stained	117 mg Wicking fluid stain

Table 8. Open Circuit Potentials (OCP) and Polarization Resistances (Rp) as Measured at Room Temperature in 3.5% Sodium Chloride Solution versus a Saturated Calomel Electrode (n = 3).

Material	*OCP (mV)*	*Rp (ohms-cm)*
4130 Steel Substrate, bare	***-756***	***$7.0x10^3$***
Baseline Coating Burnished Basecoat	***-619***	***$9.6x10^5$***
Coating A Burnished Basecoat	***-680***	***$7.1x10^4$***
Coating B Burnished Basecoat	***-1013***	***$2.6x10^4$***
Baseline Coating Burnished Basecoat + Topcoat Seal	***-754***	***$3.3x10^6$***
Coating A Burnished Basecoat + Topcoat Seal	***-613***	***$6.9x10^4$***
Coating B Burnished Basecoat + Topcoat Seal	***-746***	***$1.4x10^6$***

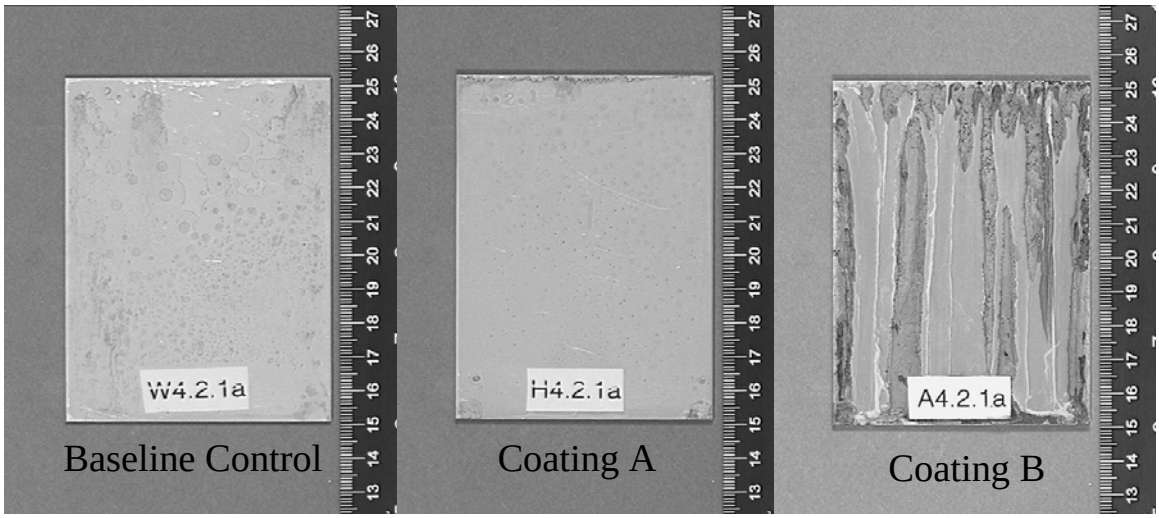

Figure 1. Optical photograph of nonscribed unburnished basecoat for baseline control, Coating A, and Coating B after 168 hours salt fog exposure.

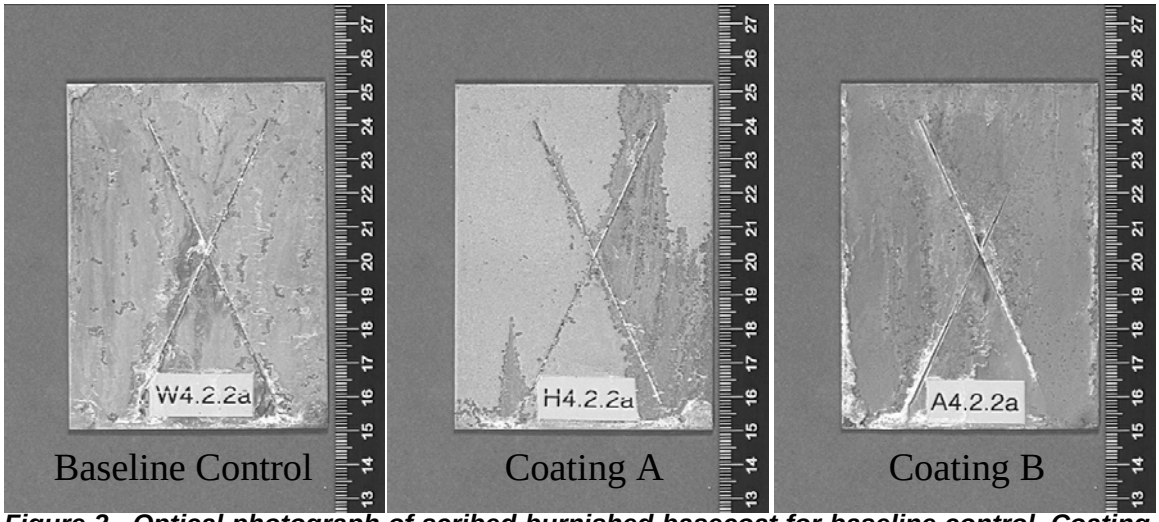

Figure 2. Optical photograph of scribed burnished basecoat for baseline control, Coating A, and Coating B after 500 hours salt fog exposure.

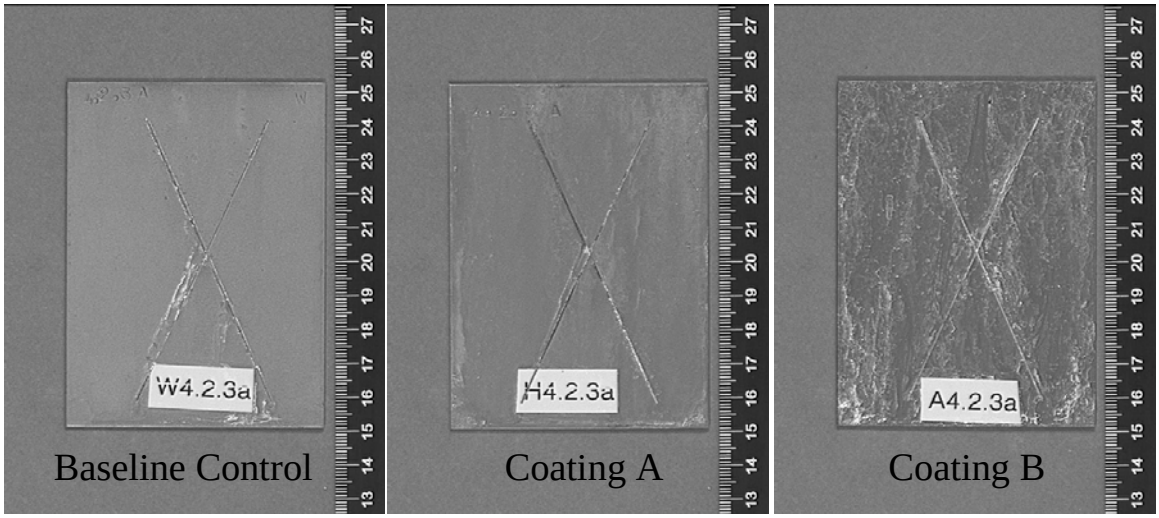

Figure 3. Optical photograph of scribed burnished basecoat with topcoat for baseline control, Coating A, and Coating B after 500 hours salt fog exposure.

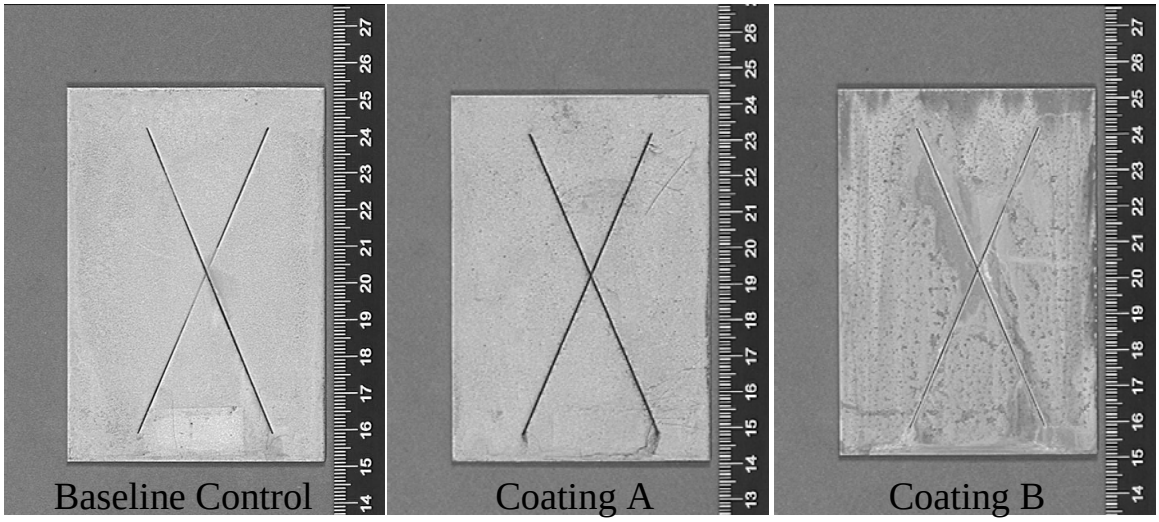

Figure 4. Optical photograph of scribed burnished basecoat for baseline control, Coating A, and Coating B after 10 cycles (one cycle = 16 hours salt fog exposure + 6 hours exposure at 750°F) exposure.

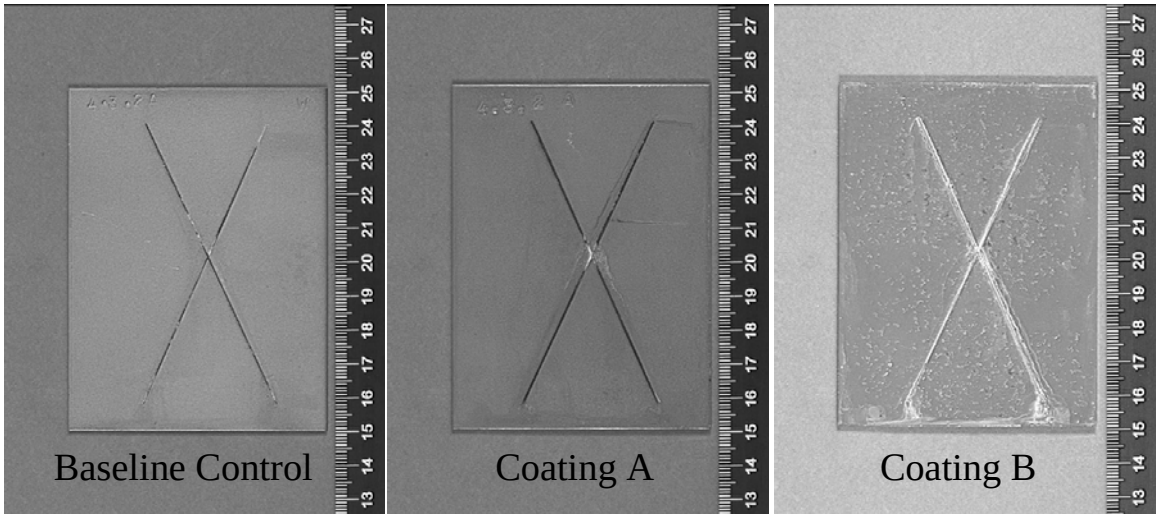

Figure 5. Optical photograph of scribed burnished basecoat with topcoat for baseline control, Coating A, and Coating B after 10 cycles (one cycle = 16 hours salt fog exposure + 6 hours exposure at 750°F) exposure.

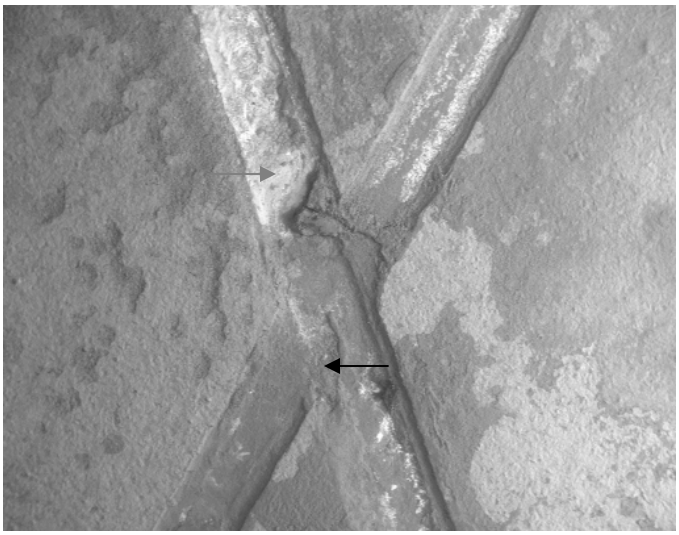

Figure 6a. SEM image of baseline control coating (in scribed condition after 500 hours salt fog exposure) taken at 10keV in backscatter mode at a magnification of 30X and a working distance of 11mm. The dark (black arrow) and light (gray arrow) areas are indicative of lighter and heavier elements, respectively.

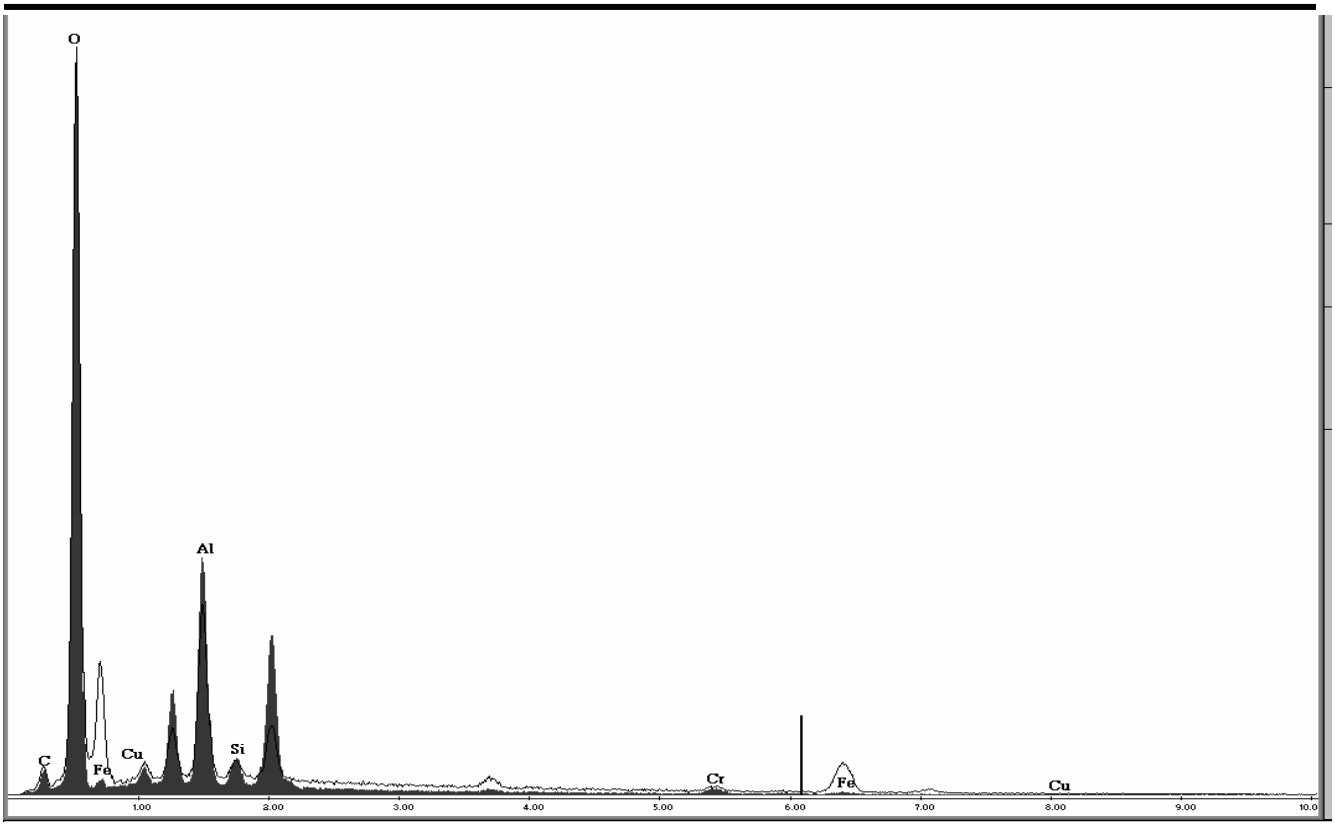

Figure 6b. EDS spectra of baseline control coating (in scribed condition after 500 hours salt fog exposure) taken at 10keV in backscatter mode. The filled curve represents the dark areas (lighter elements) in Figure 6a. The black line represents the light areas (heavier elements) in Figure 6a.

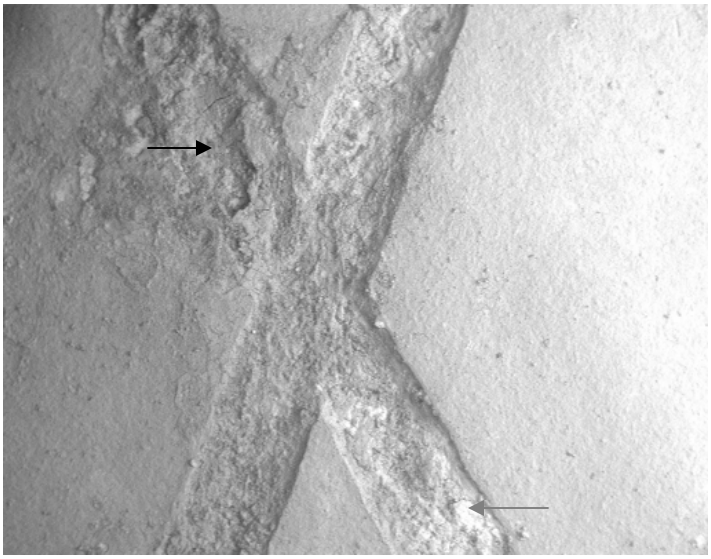

Figure 7a. SEM image of Coating A (in scribed condition after 500 hours salt fog exposure) taken at 10keV in backscatter mode at a magnification of 30X and a working distance of 11mm. The dark (black arrow) and light (gray arrow) areas are indicative of lighter and heavier elements, respectively.

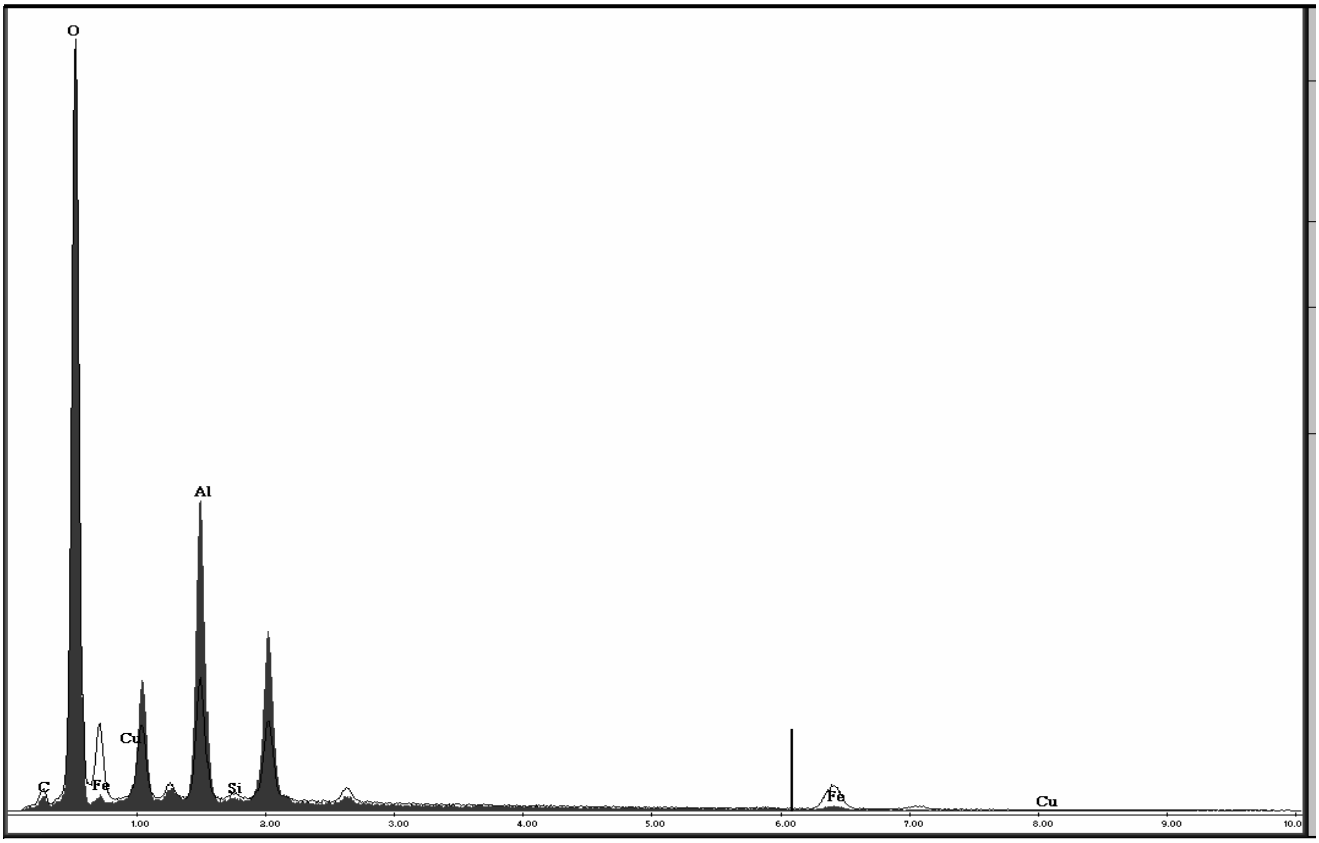

Figure 7b. EDS spectra of Coating A (in scribed condition after 500 hours salt fog exposure) taken at 10keV in backscatter mode. The filled curve represents the dark areas (lighter elements) in Figure 7a. The black line represents the light areas (heavier elements) in Figure 7a.

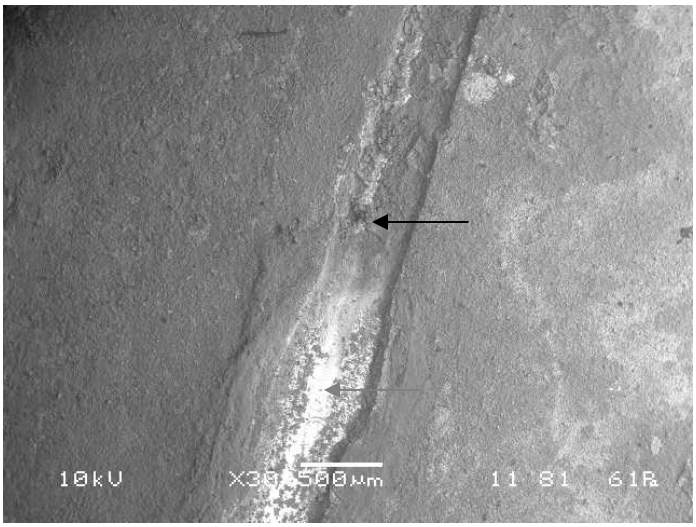

Figure 8a. SEM image of Coating B (in scribed condition after 500 hours salt fog exposure) taken at 10keV in backscatter mode at a magnification of 30X and a working distance of 11mm. The dark (black arrow) and light (gray arrow) areas are indicative of lighter and heavier elements, respectively.

Figure 8b. EDS spectra of Coating B (in scribed condition after 500 hours salt fog exposure) taken at 10keV in backscatter mode. The filled curve represents the dark areas (lighter elements) in Figure 8a. The black line represents the light areas (heavier elements) in Figure 8a.

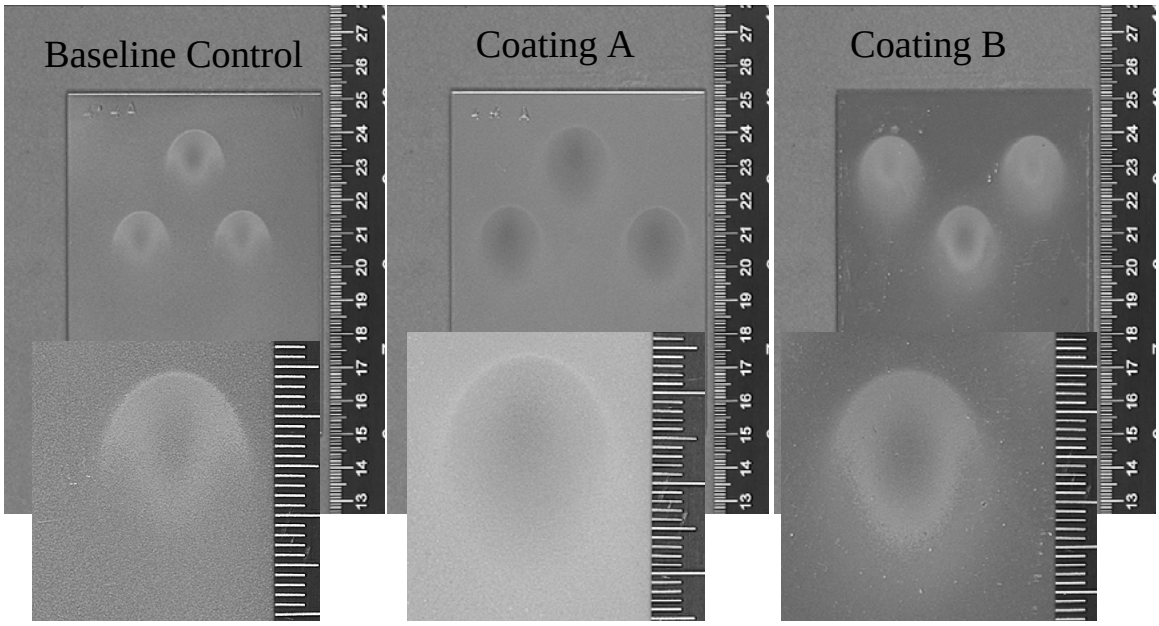

Figure 9. Optical photograph of (a) baseline control, (b) Coating A, and (c) Coating B after being subjected to falling sand.

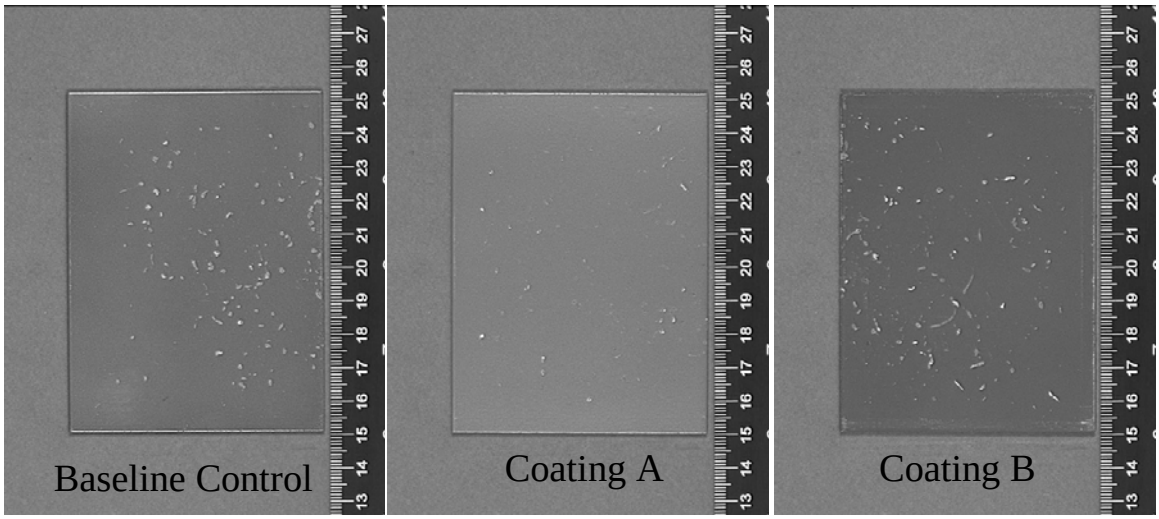

Figure 10. Optical photograph of (a) baseline control, (b) Coating A, and (c) Coating B after being subjected to impacts such as those caused by the gravelometer.

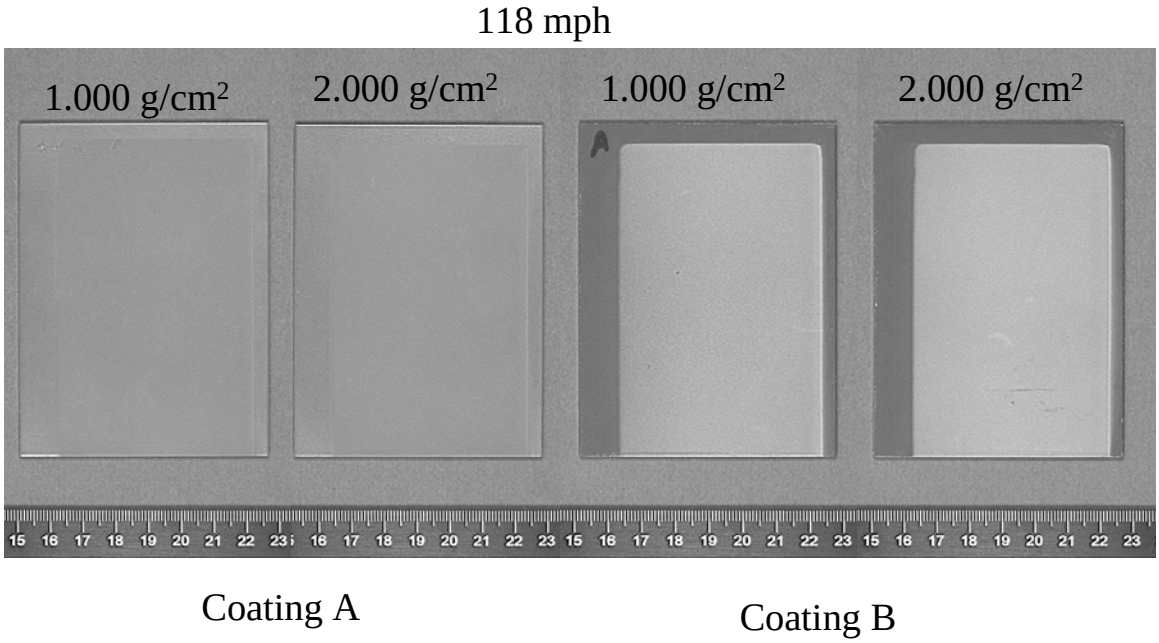

Figure 11a. Optical photographs of particle erosion results for the chromium-free alternatives at 118 mph.

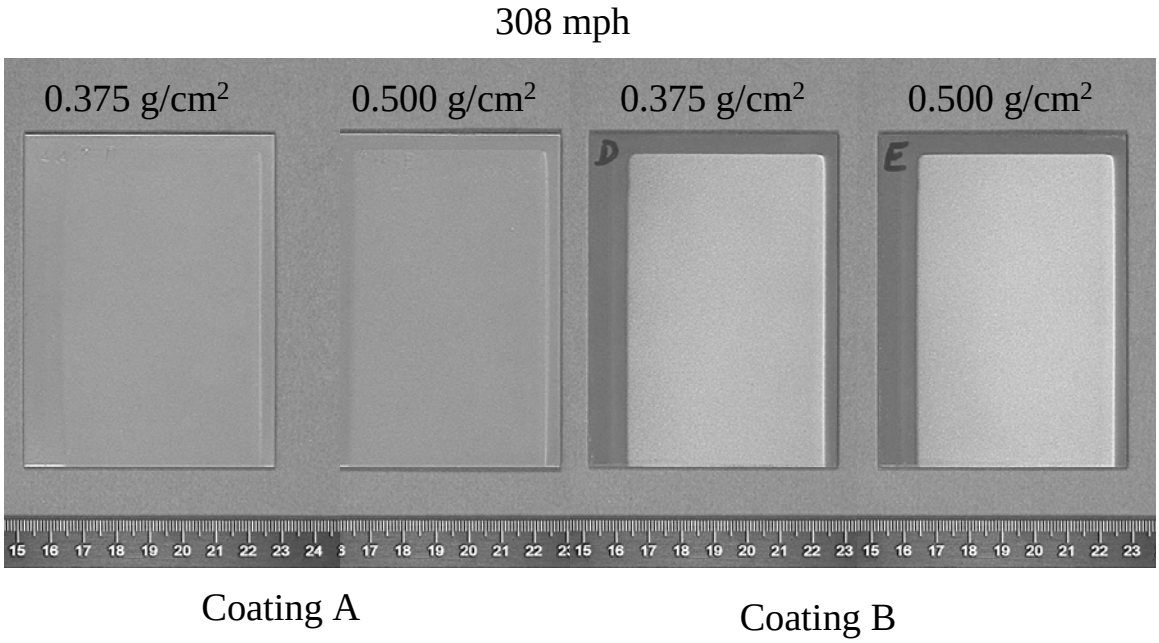

Figure 11b. Optical photographs of particle erosion results for the chromium-free alternatives at 308 mph.

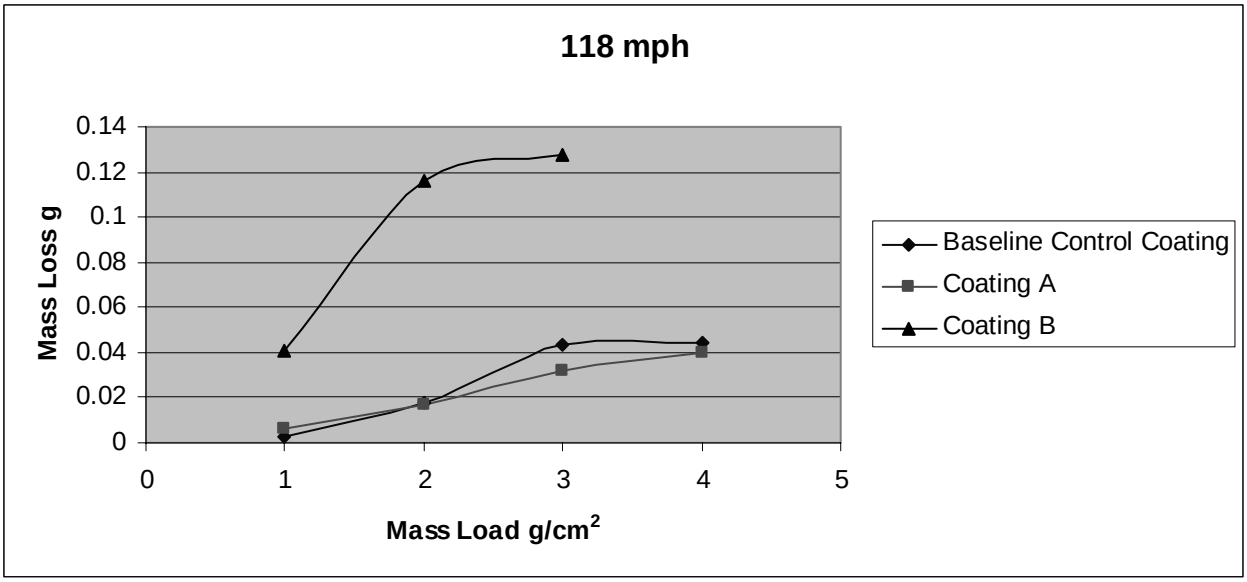

Figure 12a. Particle erosion results for the topcoated (burnished basecoat) systems at a calibrated speed of 118 mph.

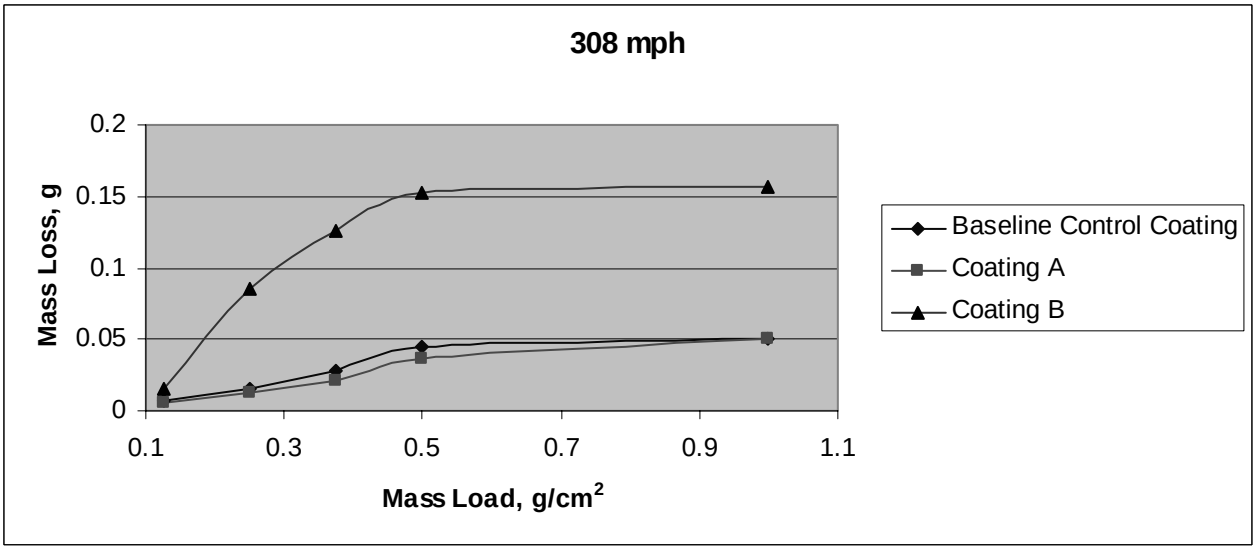

Figure 12b. Particle erosion results for the topcoated (burnished basecoat) systems at a calibrated speed of 308 mph.

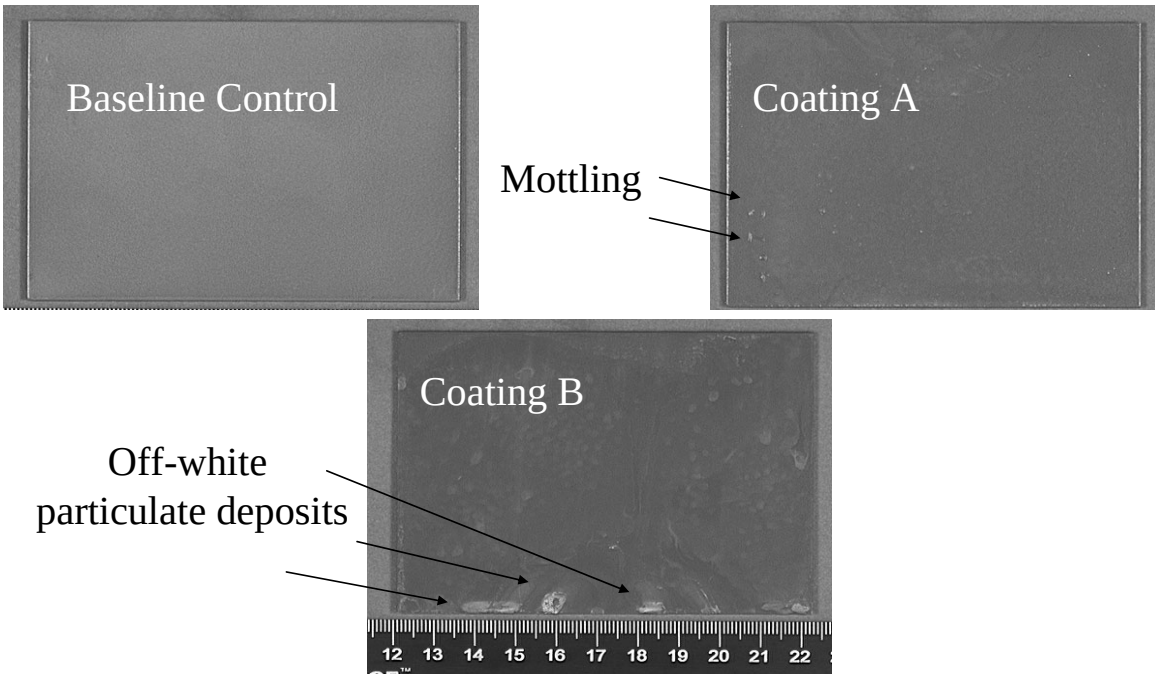

Figure 13. Optical photographs of (a) baseline control, (b) Coating A, and (c) Coating B after30 days humidity exposure at a relative humidity (RH) of 95% and temperature of 140 ℉.

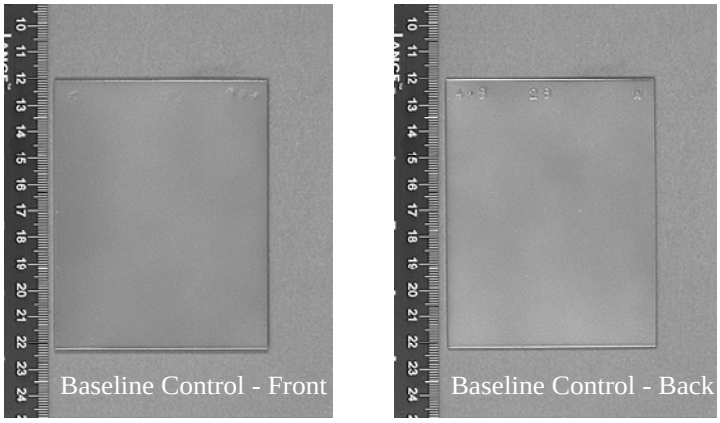

(a)

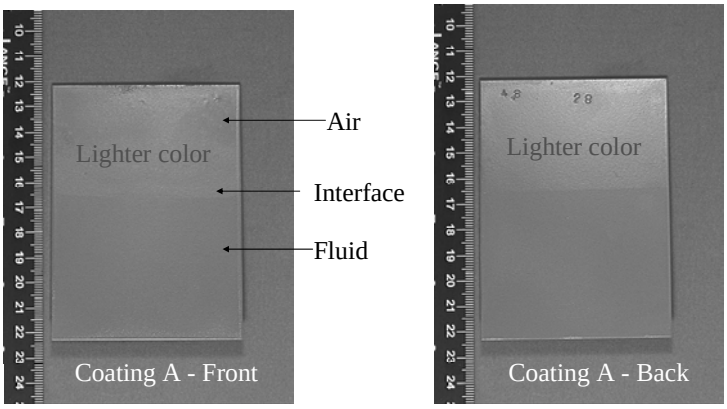

(b)

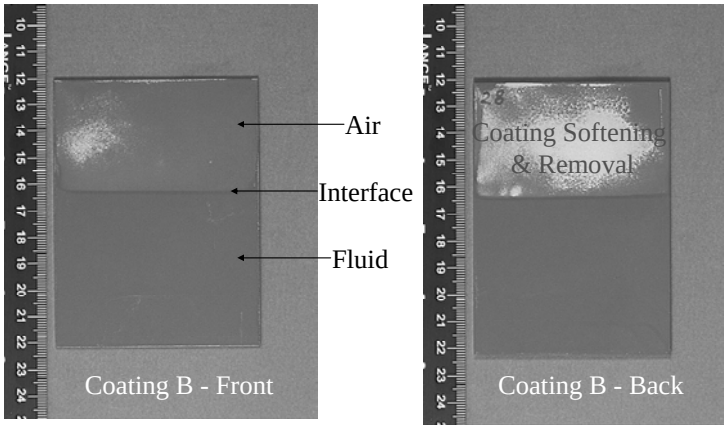

(c)

Figure 14. Optical photograph of (a) baseline control, (b) Coating A, and (c) Coating B after 24 hours fluid immersion in 120 degree Fahrenheit distilled water.

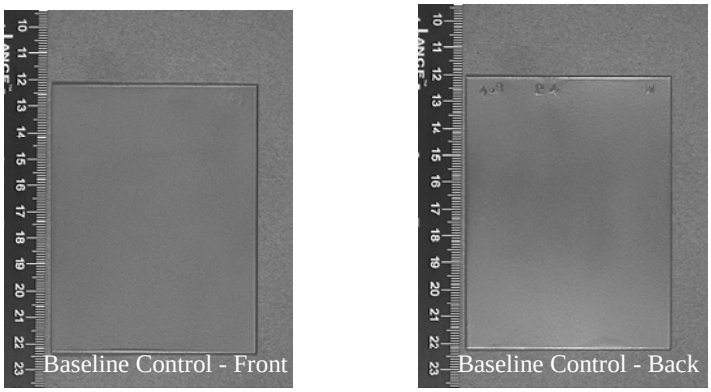

No visible fluid line of demarcation

(a)

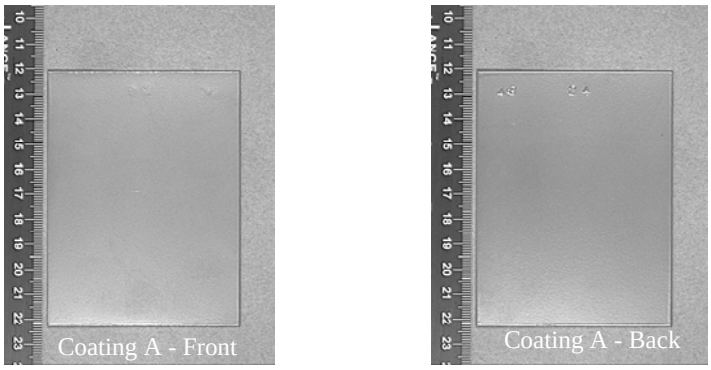

No visible fluid line of demarcation

(b)

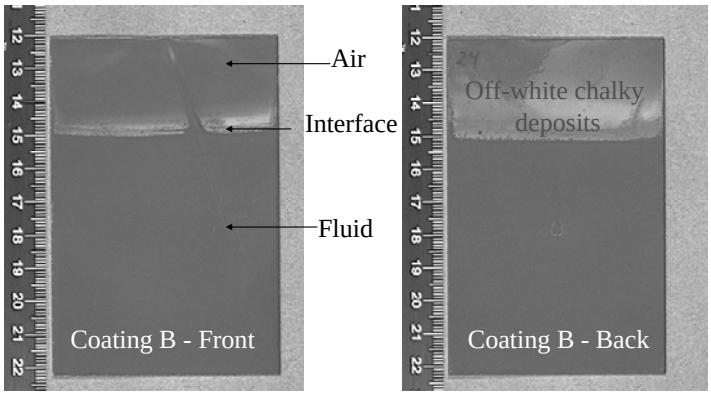

(c)

Figure 15. Optical photograph of (a) baseline control, (b) Coating A, and (c) Coating B after 8 hours fluid immersion in 400 degree Fahrenheit engine lubricating oil.

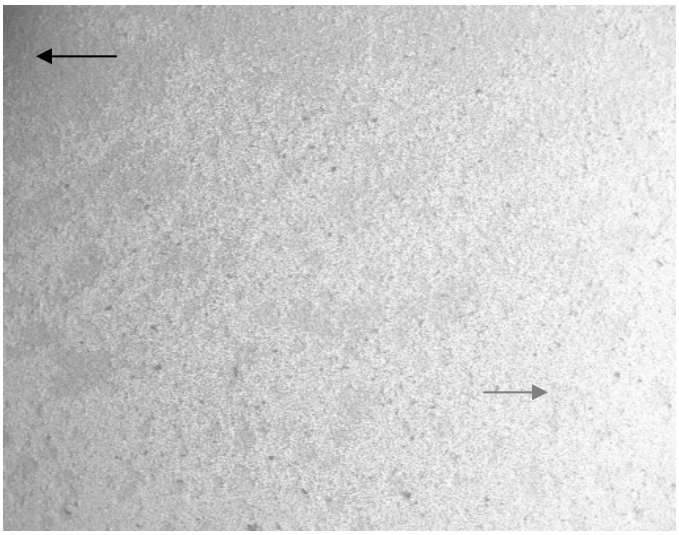

Figure 16a. SEM image of Coating B after hot water immersion taken at 10keV in backscatter mode at a magnification of 30X and a working distance of 11mm. The dark (black arrow) and light (gray arrow) areas are indicative of lighter and heavier elements, respectively.

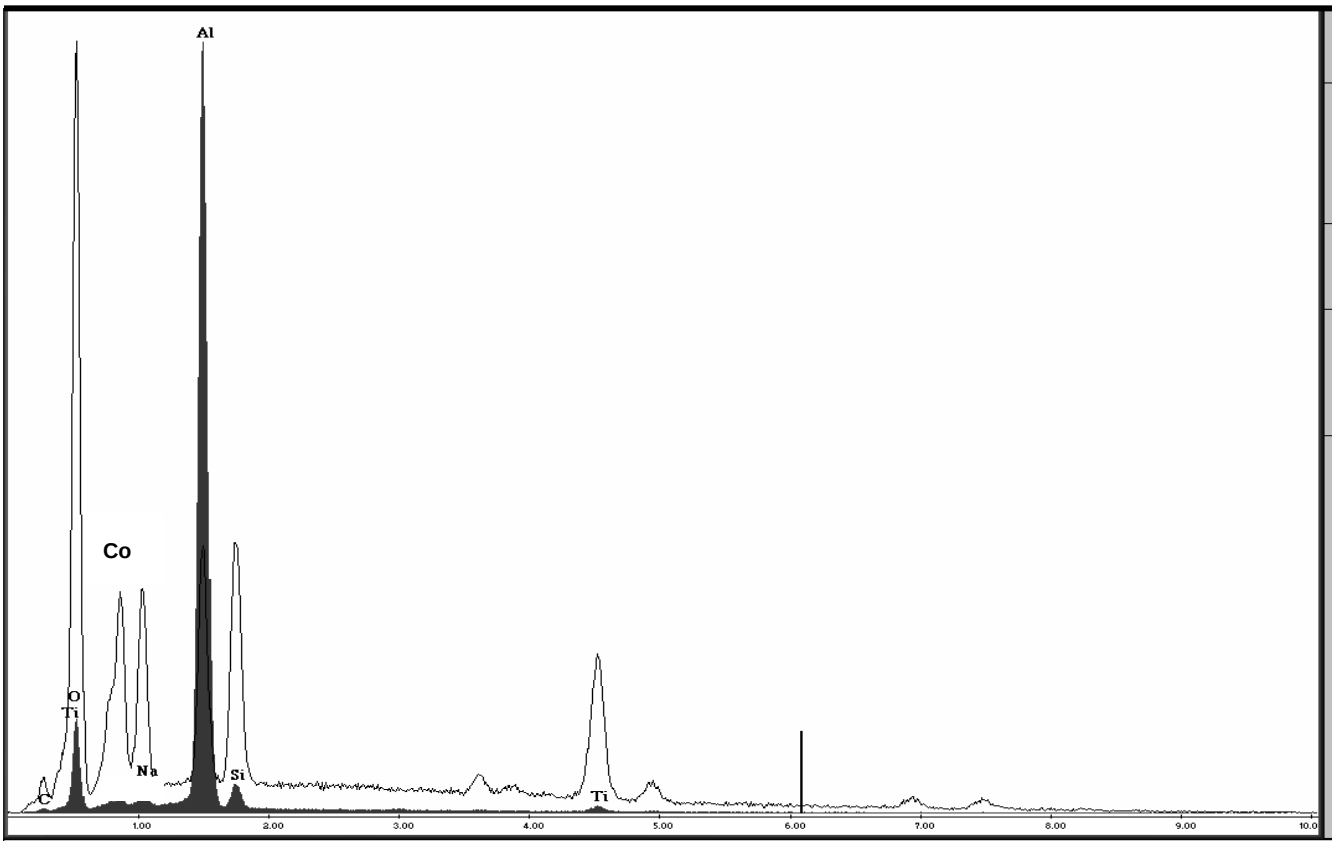

Figure 16b. EDS spectra of Coating B taken at 10keV in backscatter mode. The filled curve represents the dark areas (lighter elements) in Figure 15a. The black line represents the light areas (heavier elements) in Figure 15a.

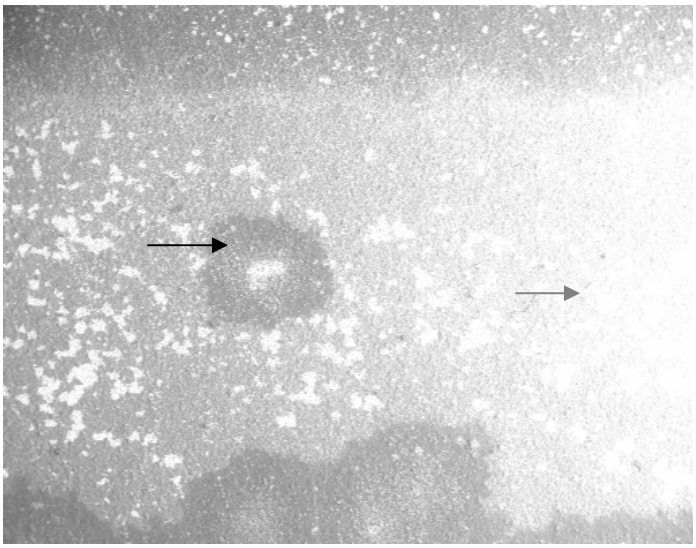

Figure 17a. SEM image of Coating B after hot oil immersion taken at 10keV in backscatter mode at a magnification of 30X and a working distance of 11mm. The dark (black arrow) and light (gray arrow) areas are indicative of lighter and heavier elements, respectively.

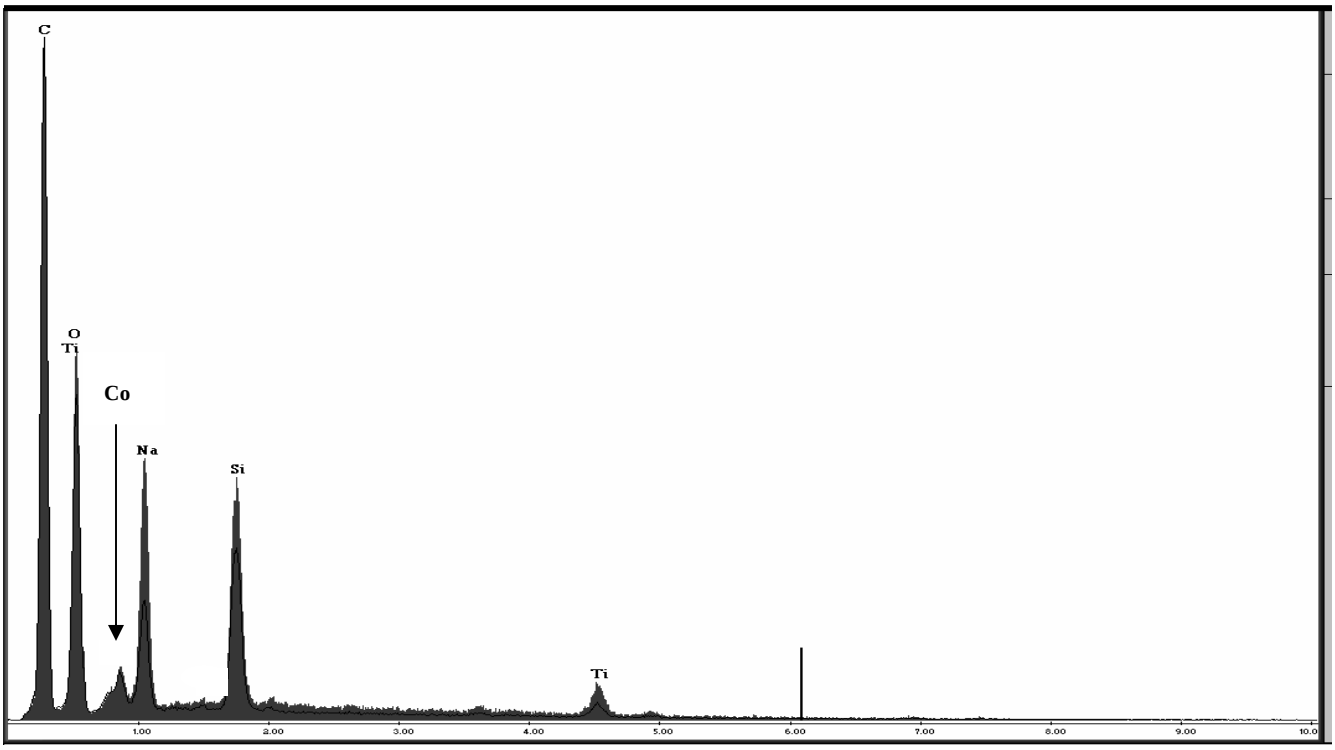

Figure 17b. EDS spectra of Coating B taken at 10keV in backscatter mode. Identical spectra were generated for the light and dark areas, thus only one curve is presented here. The filled curve shown is taken from the dark areas (lighter elements) in Figure 17b.

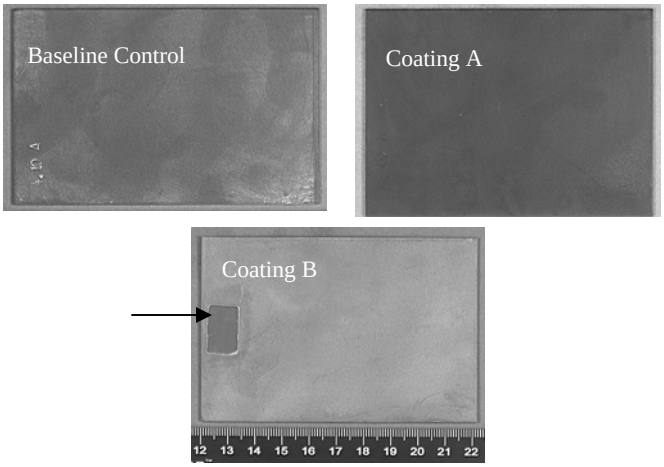

Figure 18. Visual photograph of panels after coating removal using individual coating stripping procedures outlined in Table 2. A mask was used on a portion of coating B to be used as a marker (black arrow) of coating thickness.